Univerza v Ljubljani
Fakulteta za strojništvo

Kako izboljšati zmogljivosti motorjev z notranjim zgorevanjem?

Tomaž Katrašnik

Univerza v Ljubljani

Fakulteta za strojništvo

Laboratorij za toplotne batne stroje

Razvrstitev motorjev z notranjim zgorevanjem

Batni Motorji z Notranjim Zgorevanjem - BMNZ

www3.mercedes-benz.com

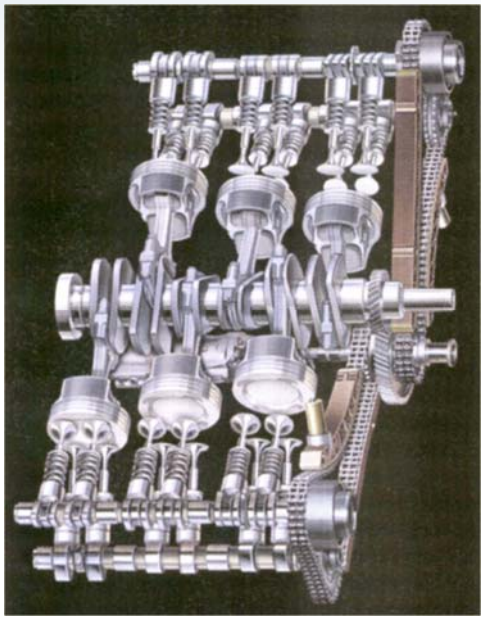

www.porsche.com

Turbinski Motorji z Notranjim Zgorevanjem - TMNZ

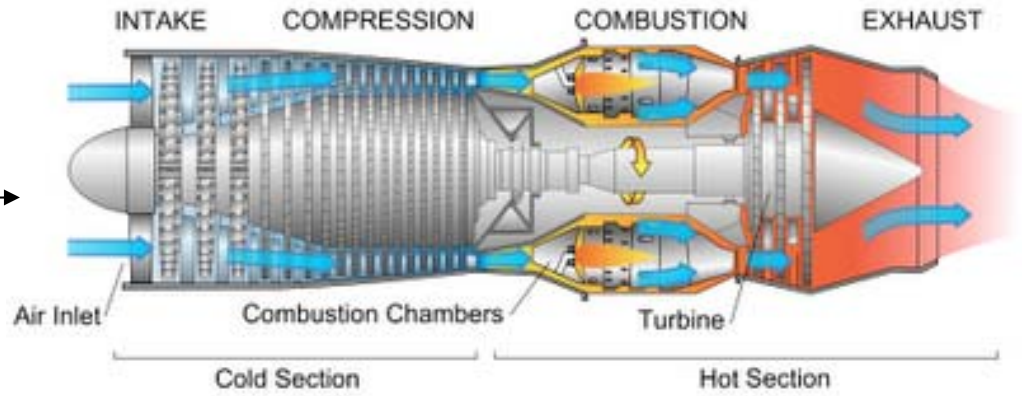

www.adl.gatech.edu

Transport in EU25

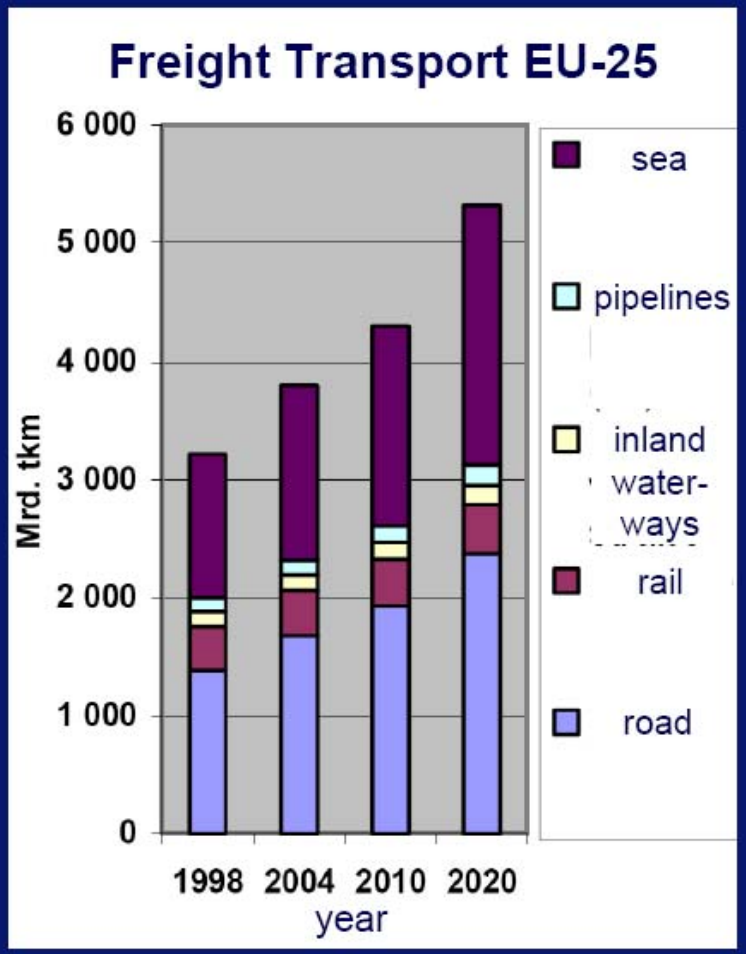

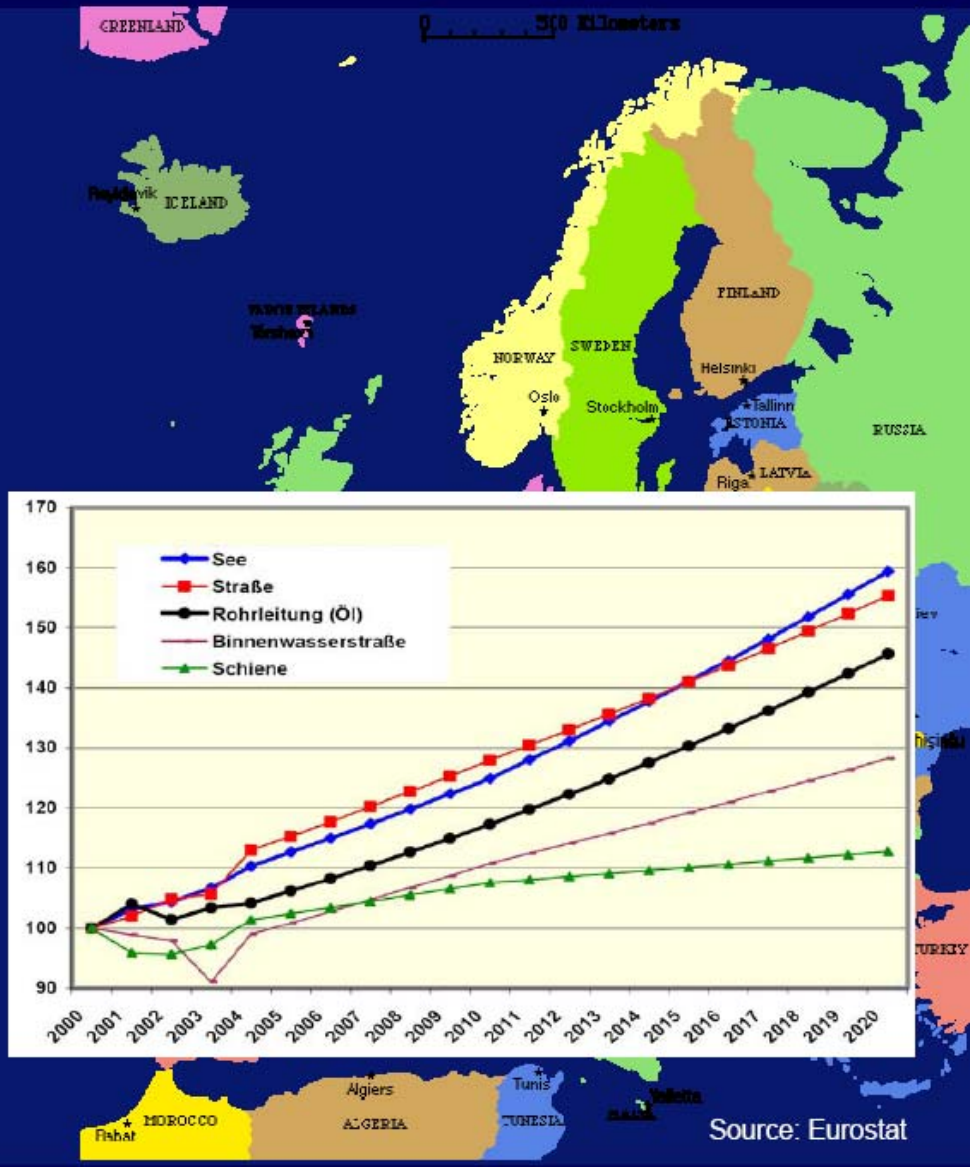

Source: Eurostat

CO_2 Emissions in the EU

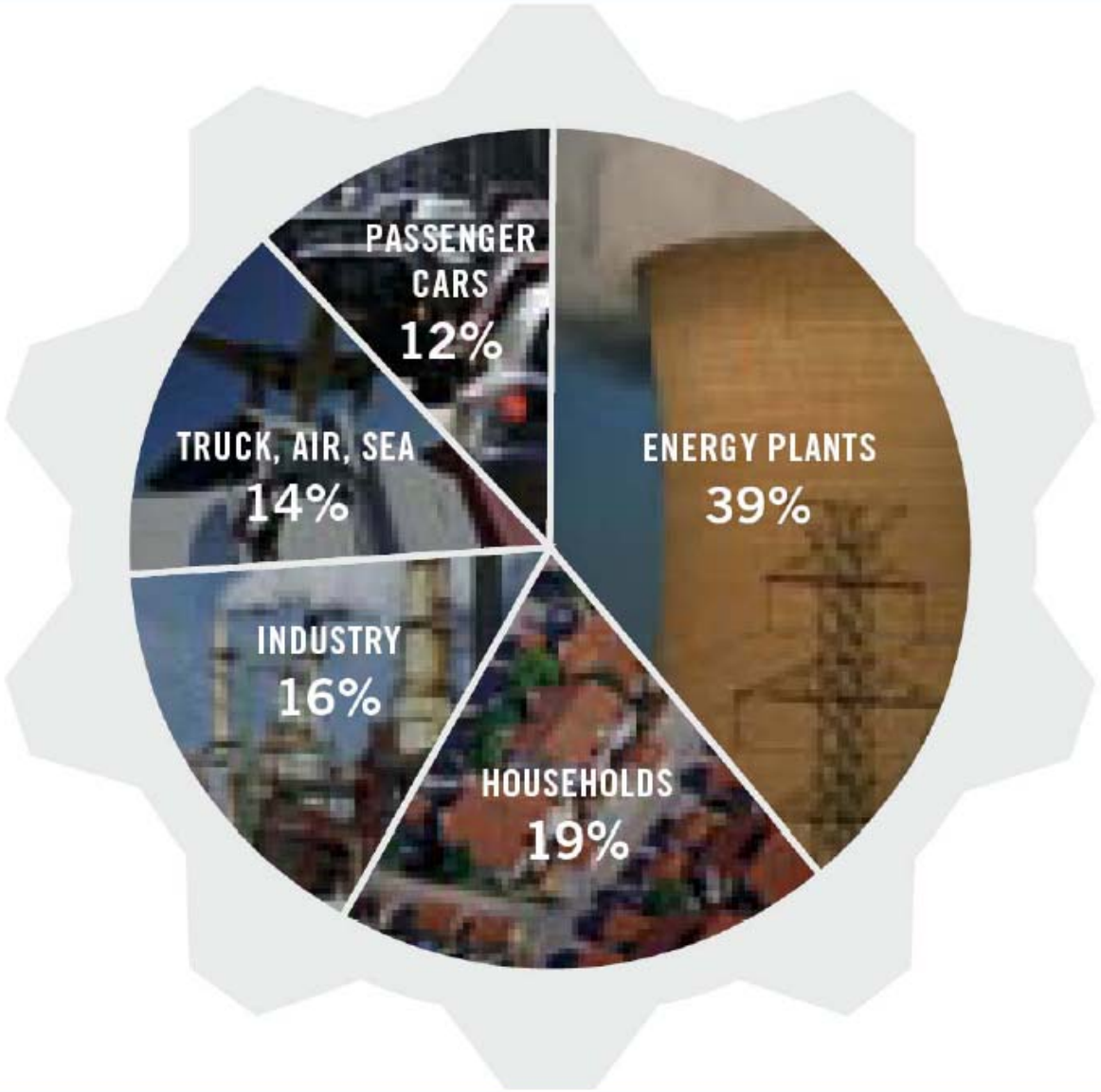

Source: ACEA, EC, 2004

Fuel Supply Forecast

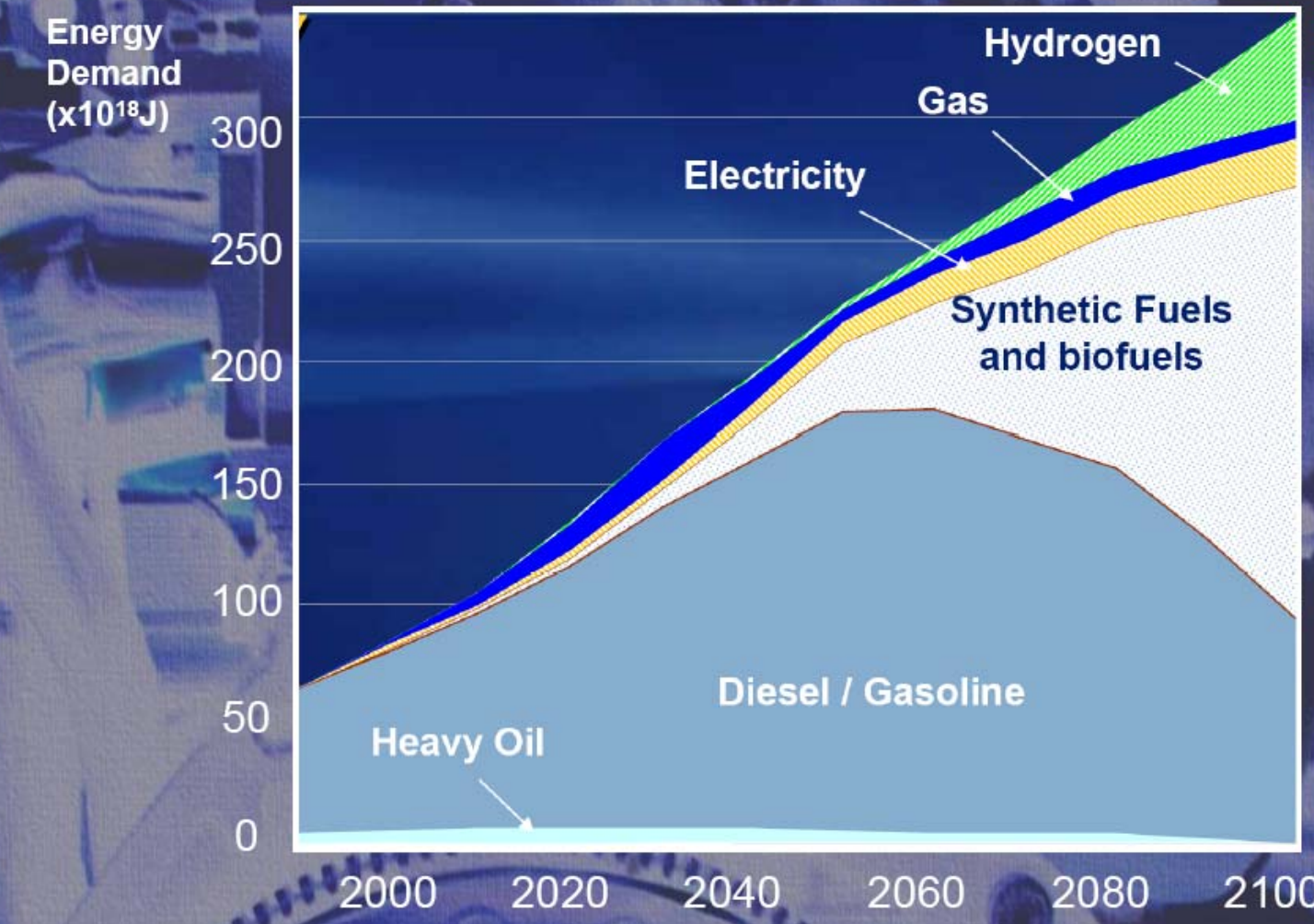

Source: GM

Roadmap "Universal Powertrain"

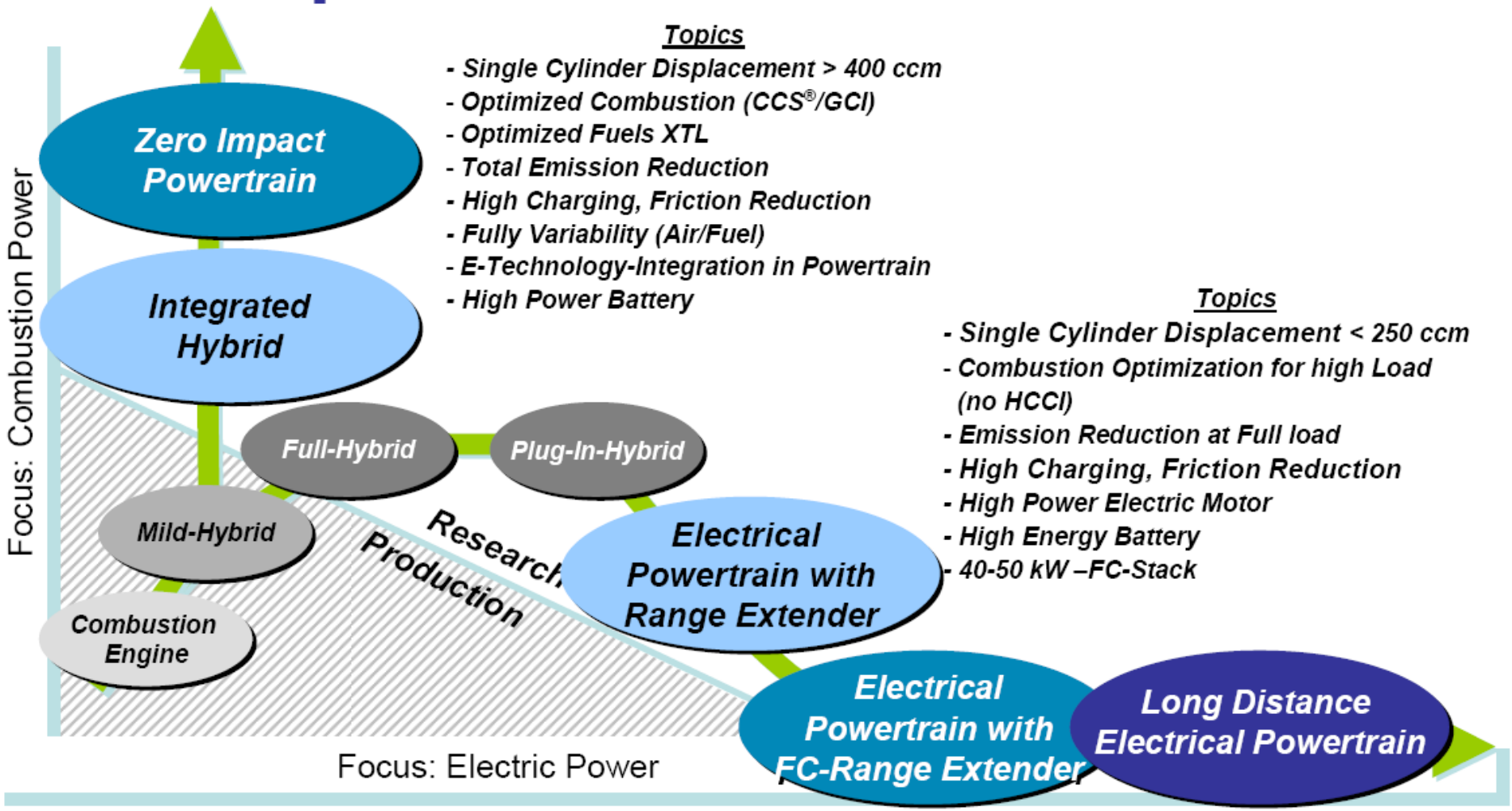

CO_2 Emission – European Scenario

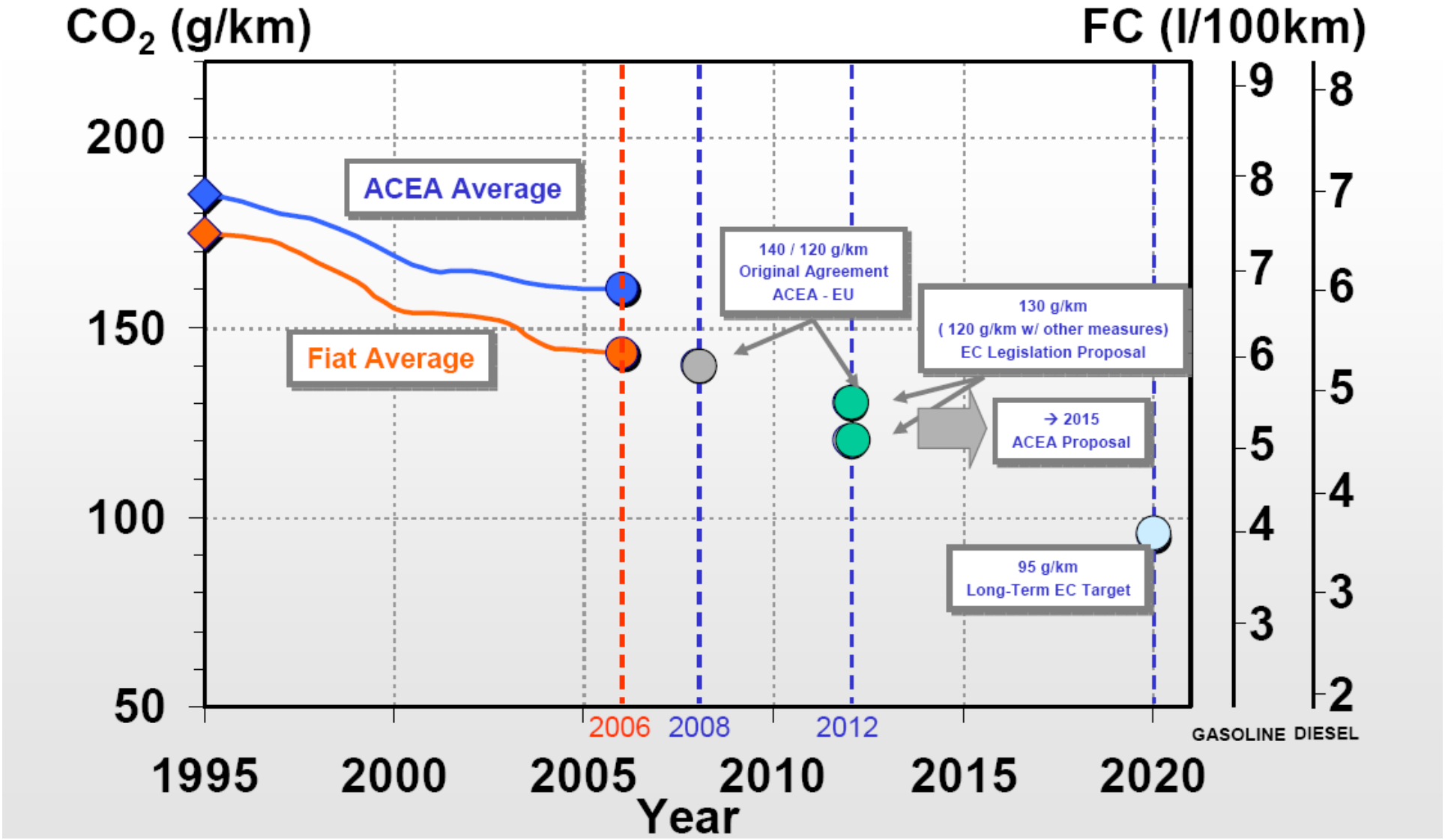

Shema Ottovega motorja

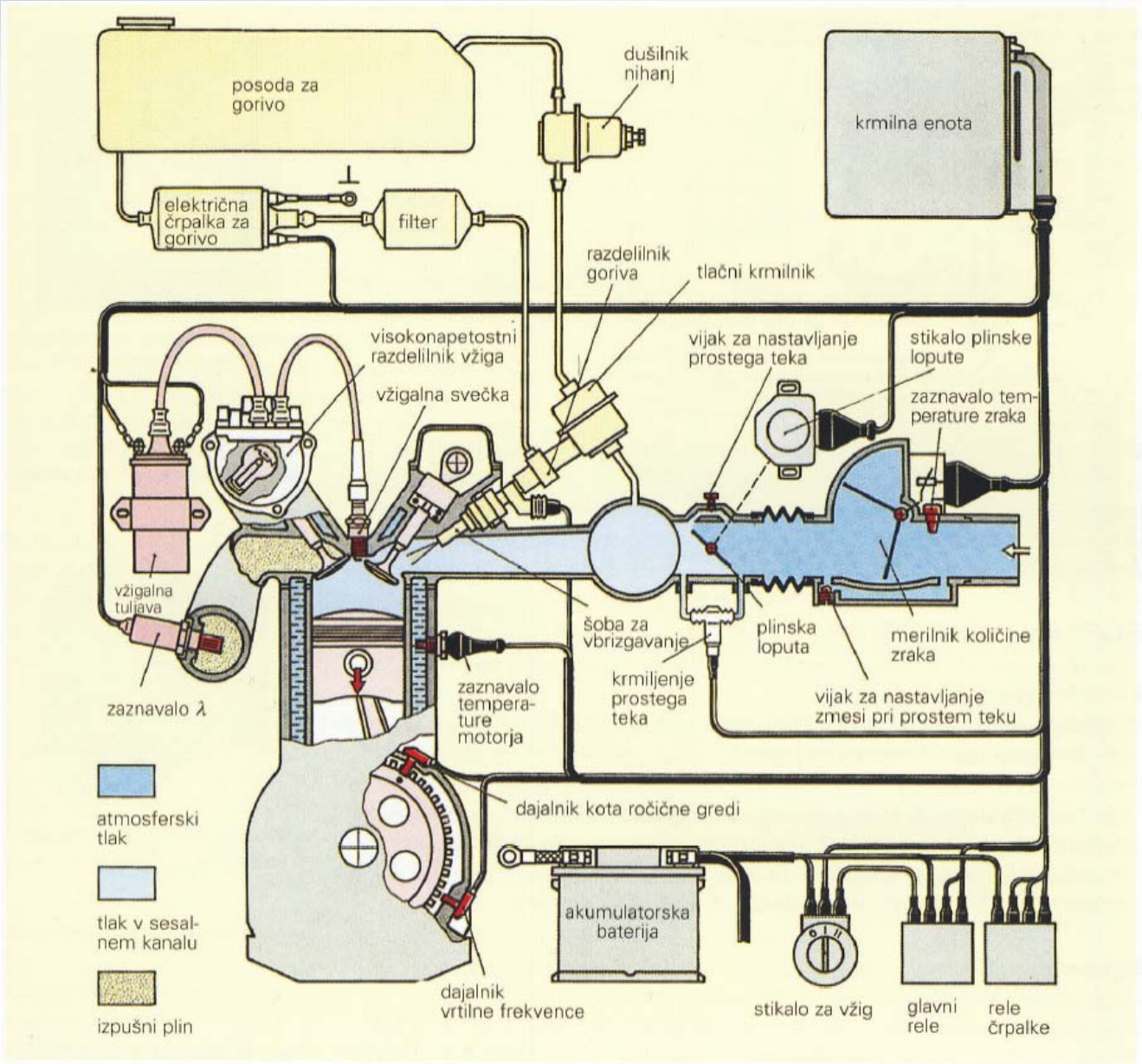

Vir: Motorno vozilo, 2004

Stehiometrično razmerje

Masa kisika, ki je potrebna za zgorevanje goriva, sestavljenega iz ogljika, vodika, žvepla in kisika:

$$O_{st} = 32.00\left(\frac{c}{12.01} + \frac{h}{4.032} + \frac{s}{32.06} - \frac{o}{32.00}\right) \qquad \left(\frac{\text{kg kisika}}{\text{kg goriva}}\right)$$

c - masni delež ogljika v gorivu

h - masni delež vodika v gorivu

s - masni delež žvepla v gorivu

o - masni delež kisika v gorivu

Ob upoštevanju masnega deleža kisika v zraku

$$L_{st} = \frac{O_{st}}{0.232}$$

izračunamo maso zraka, ki je potrebna za stehiometrično zgorevanje

$$L_{st} = 137.85\left(\frac{c}{12.01} + \frac{h}{4.032} + \frac{s}{32.06} - \frac{o}{32.00}\right) \qquad \left(\frac{\text{kg zraka}}{\text{kg goriva}}\right)$$

Meje vnetljivosti homogene zmesi

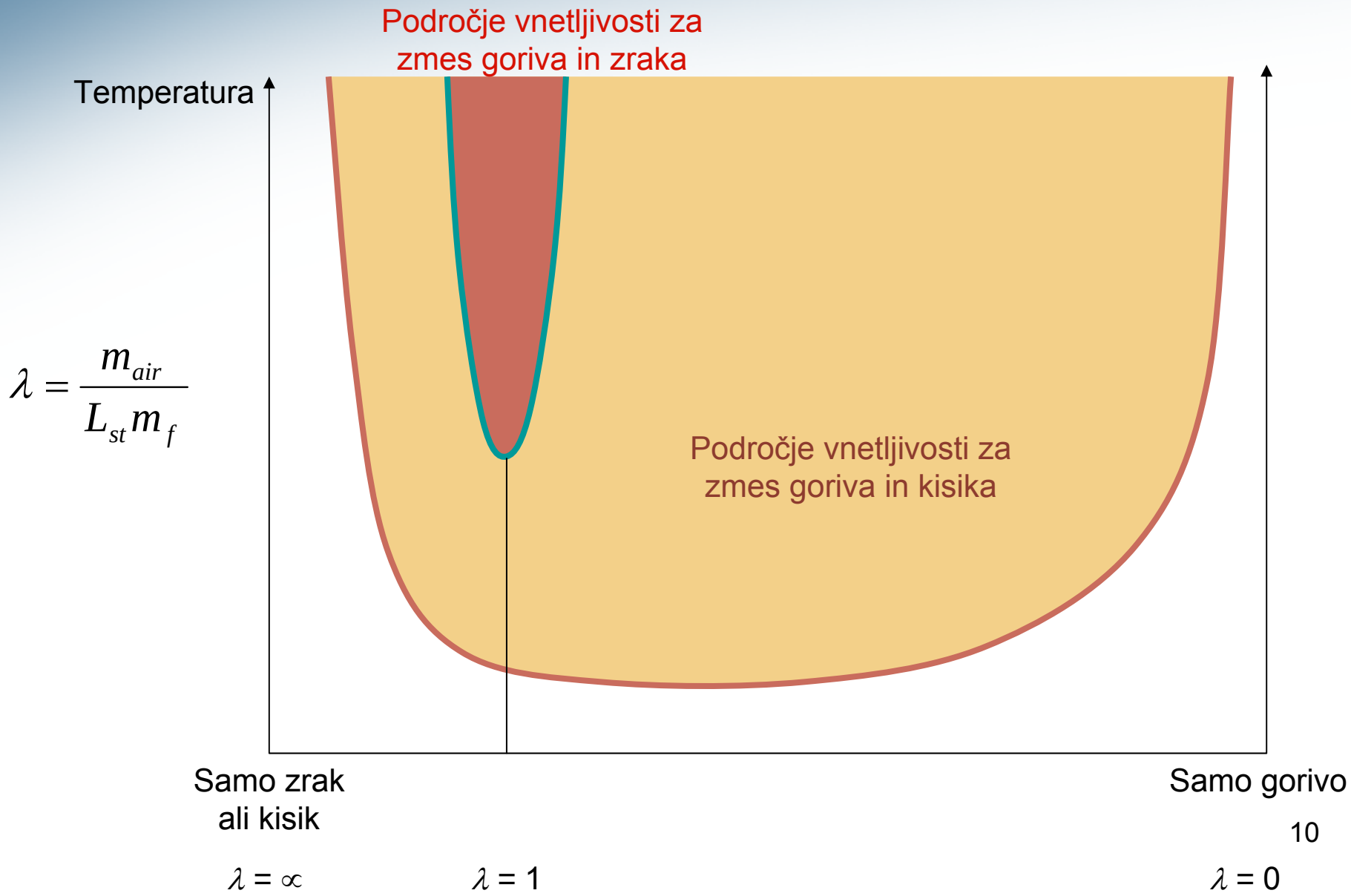

$$\lambda = \frac{m_{air}}{L_{st} m_f}$$

Mešalna razmerja Ottovih motorjev

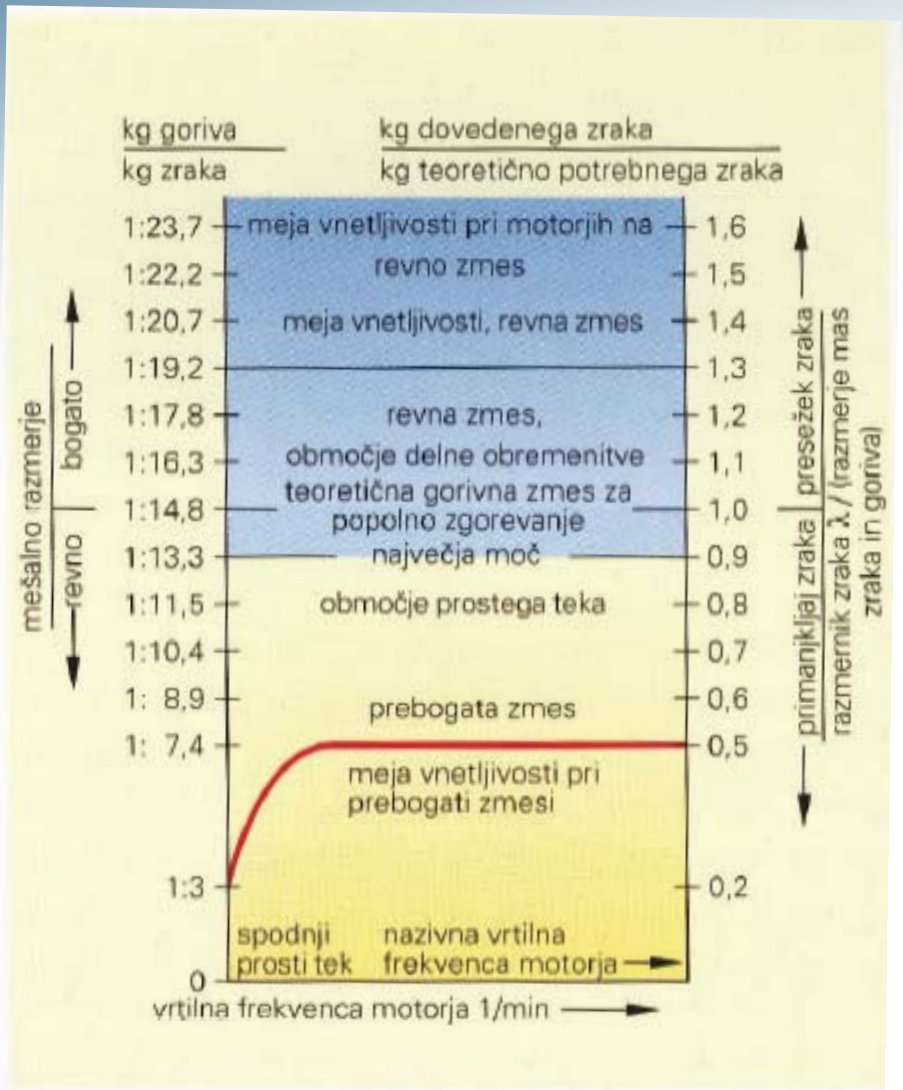

Slika 2.1.12-1: Mešalna razmerja, razmernik zraka

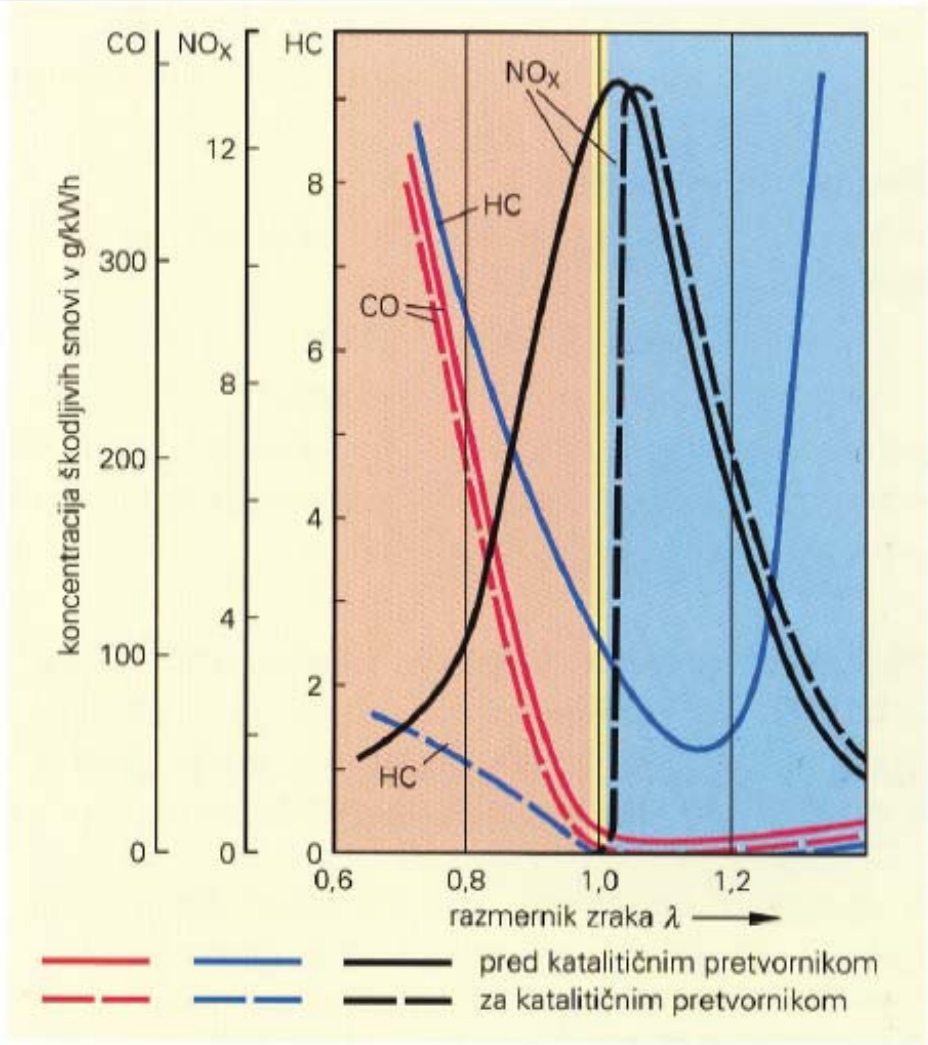

Slika 2.1.15-6: Zmanjšanje škodljivih snovi pri različnih vrednostih razmernika zraka

Vir: Motorno vozilo, 2004

Dizelsko zgorevanje

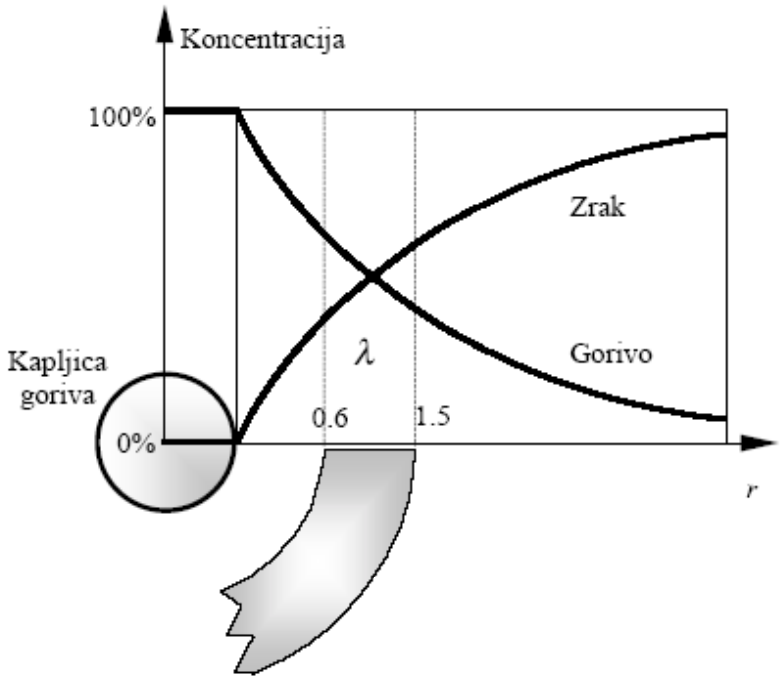

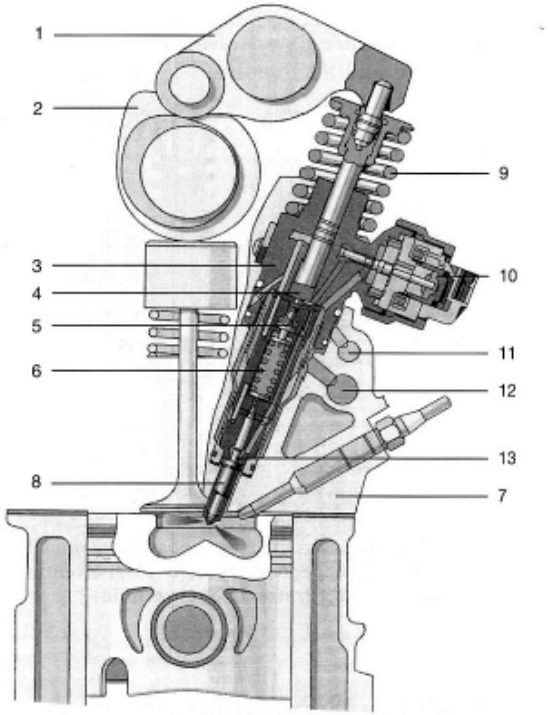

$$\lambda = \frac{m_{air}}{L_{st} m_f} \qquad \lambda_{Diesel} > 1$$

Kurilna vrednost goriva in stehiometrične zmesi

$$H_{mix} = \frac{\eta_{comb} H_{LHV}}{1 + \lambda L_{st}}$$

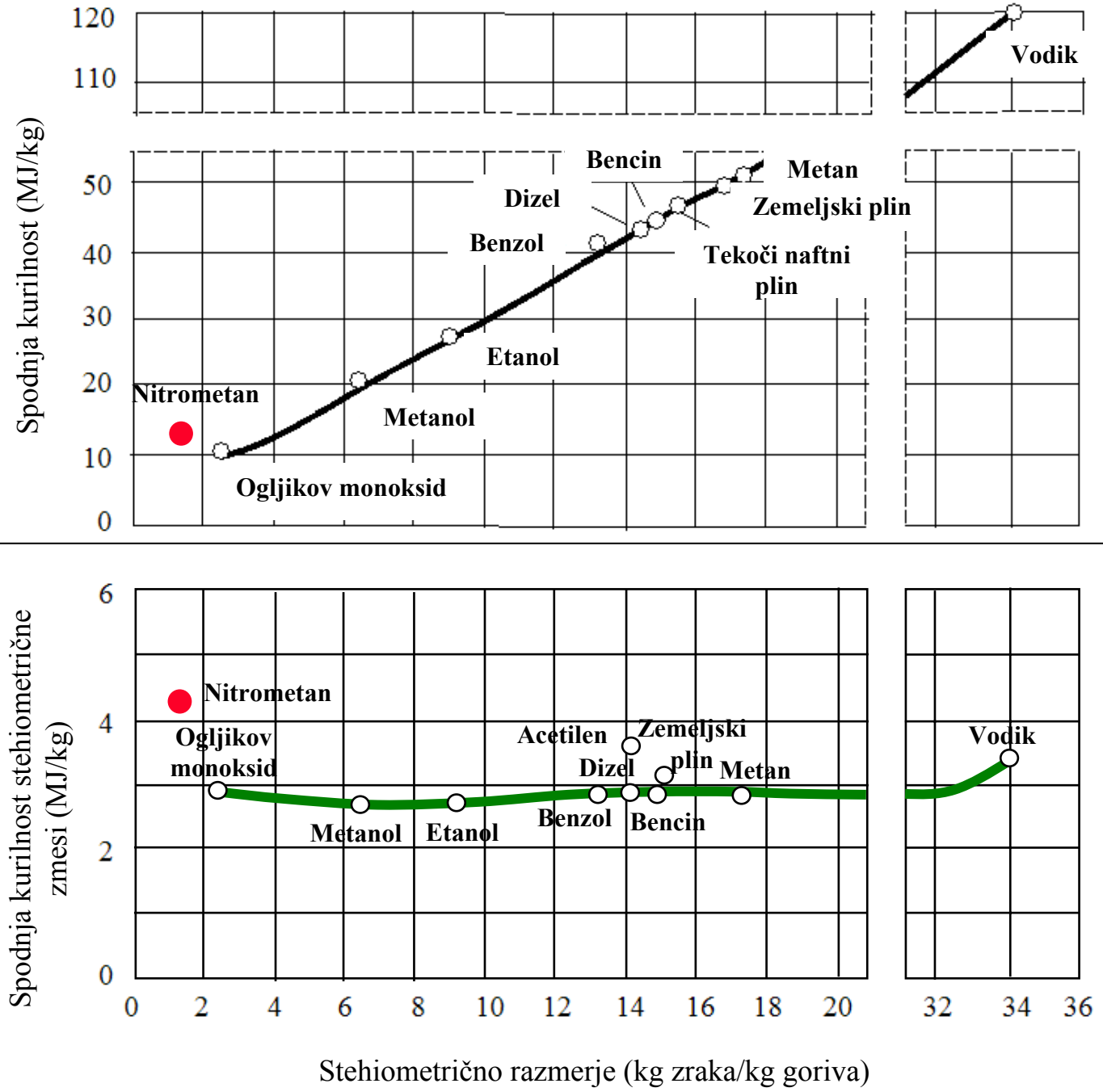

Izkoristek in specifična poraba

Izkoristek:

$$\eta = \frac{W}{Q_{dovedena}} = \frac{Q_{dovedena} - Q_{odvedena}}{Q_{dovedena}} = \frac{W}{m_{goriva} H_k}$$

$$W = \oint p \mathrm{d}V$$

Specifična poraba:

$$b = \frac{m_{goriva}}{W} = \frac{1}{\eta H_k}$$

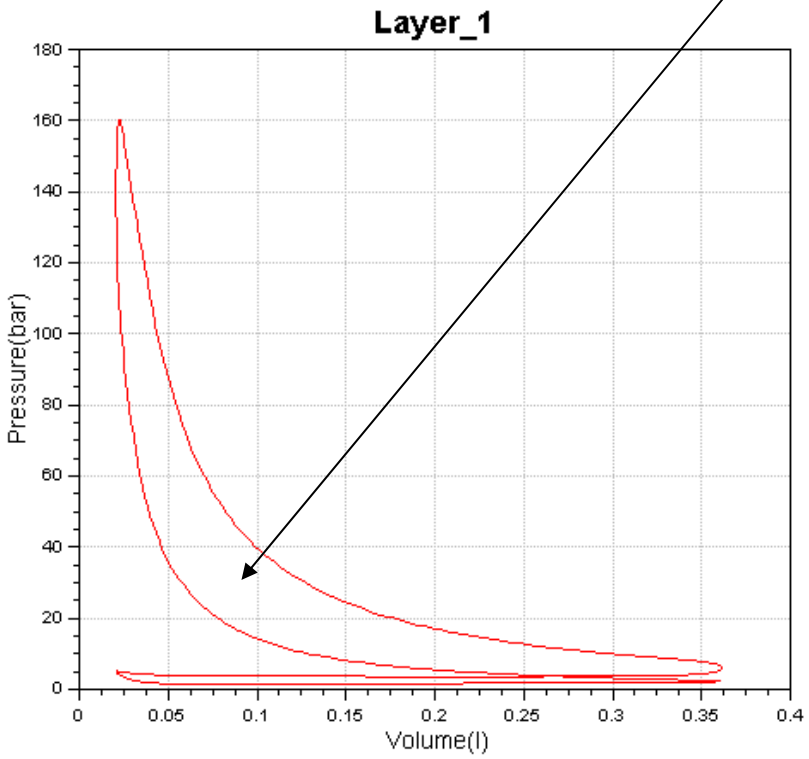

Delovna sposobnost

Srednji efektivni tlak:

$$p_{eff} = \frac{N_{st} W}{V_g} = \frac{N_{st} \oint p \mathrm{d}V}{V_g}$$

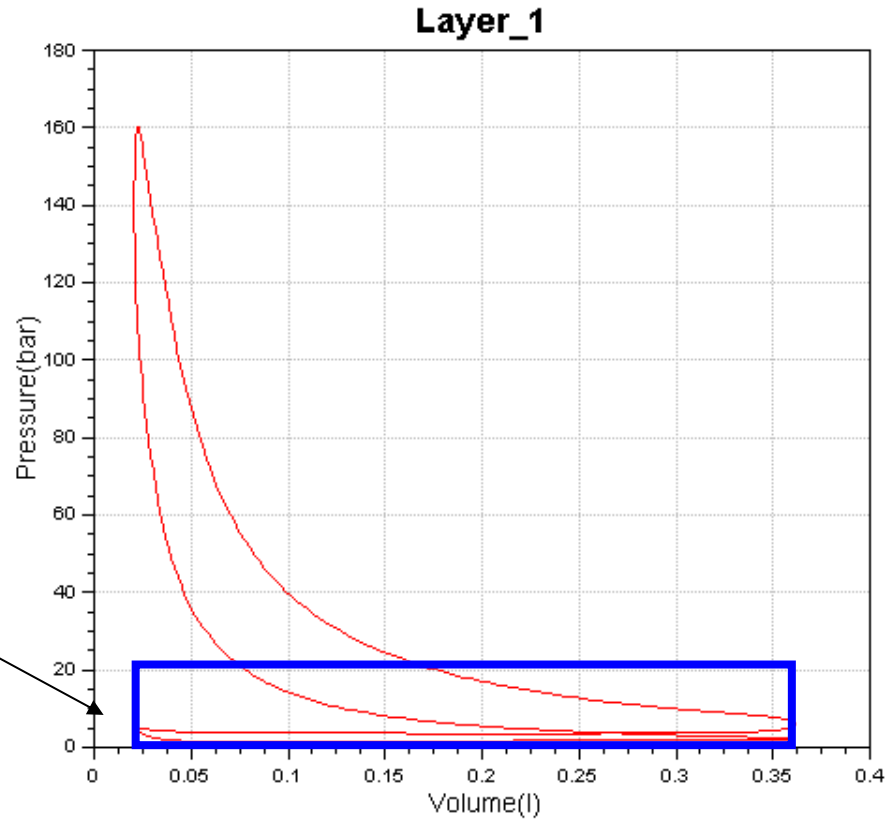

$N_{st} = 2$ ... 4T

$N_{st} = 1$ ... 2T

Primerjava realnega in teoretičnega 4T cikla

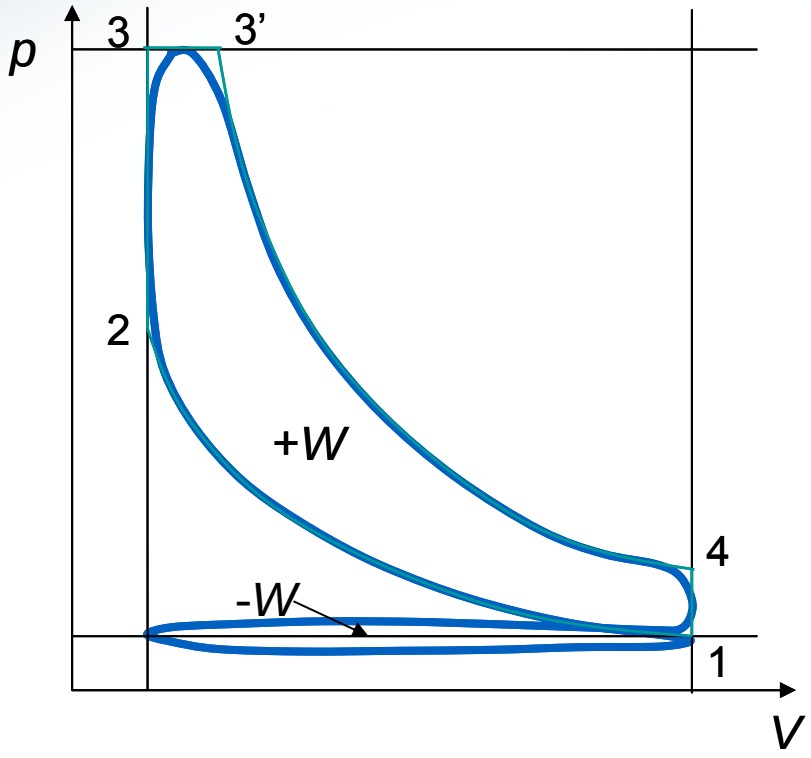

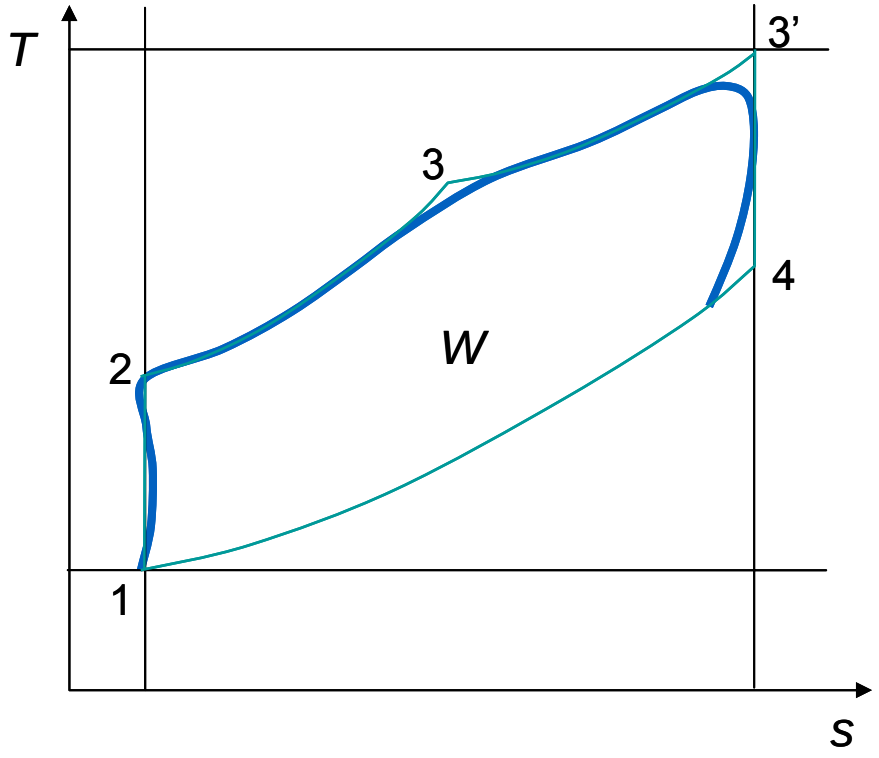

Izkoristki MNZ

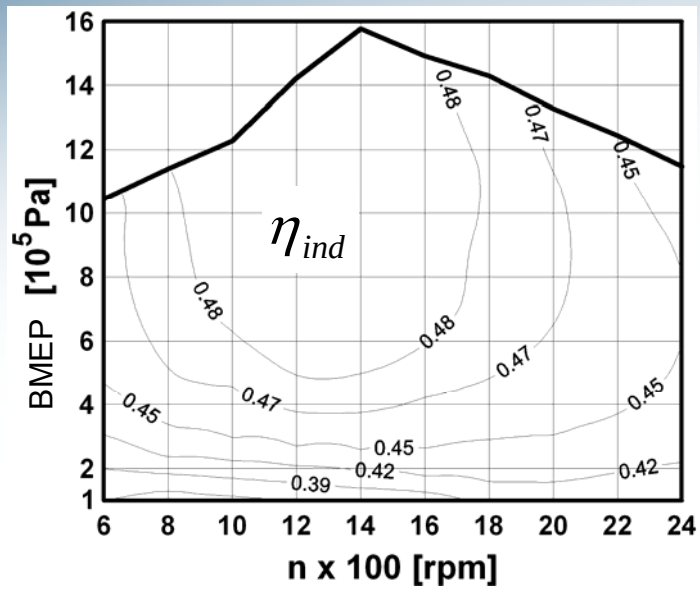

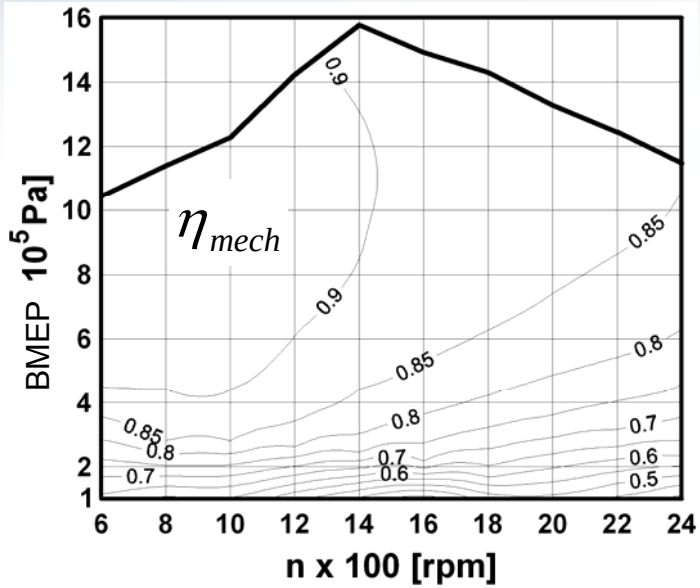

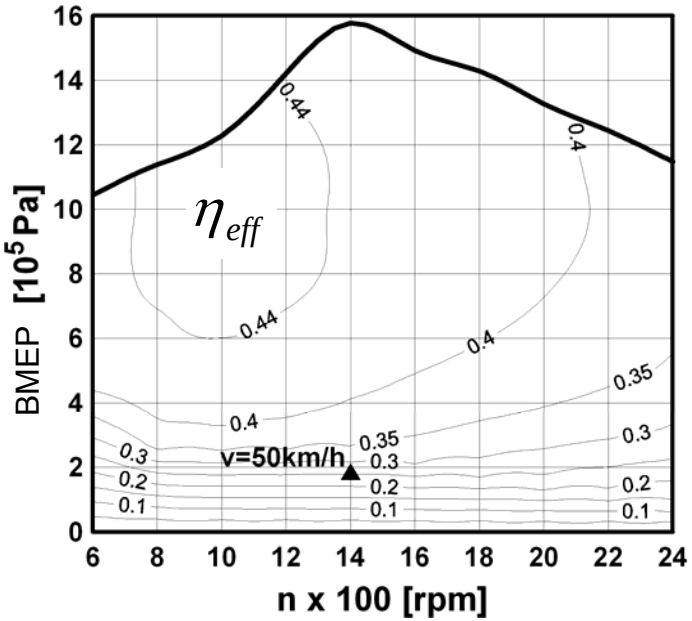

$$\eta_{eff} = \eta_{ind}\eta_{mech}$$

Teoretični cikli v BMNZ

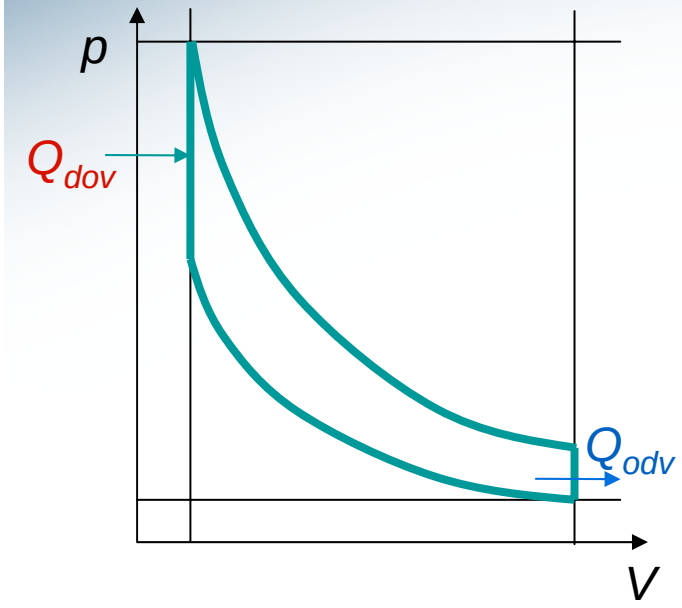

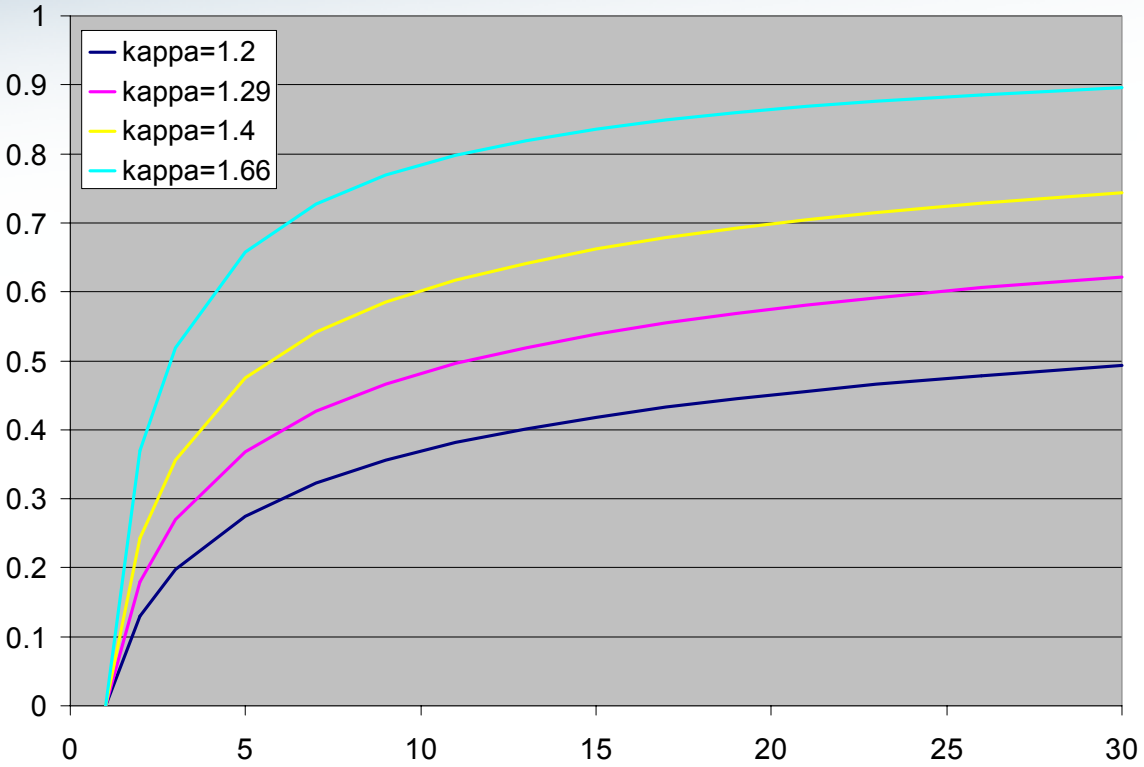

$$\eta = 1 - \frac{1}{\varepsilon^{\kappa-1}}$$

$$p_{eff} = \frac{p_1}{c_v T_1} \frac{m_f H_{LHV}}{m} \frac{\varepsilon}{\varepsilon - 1} \frac{1}{\kappa - 1} \eta$$

Spremenljivo kompresijsko razmerje

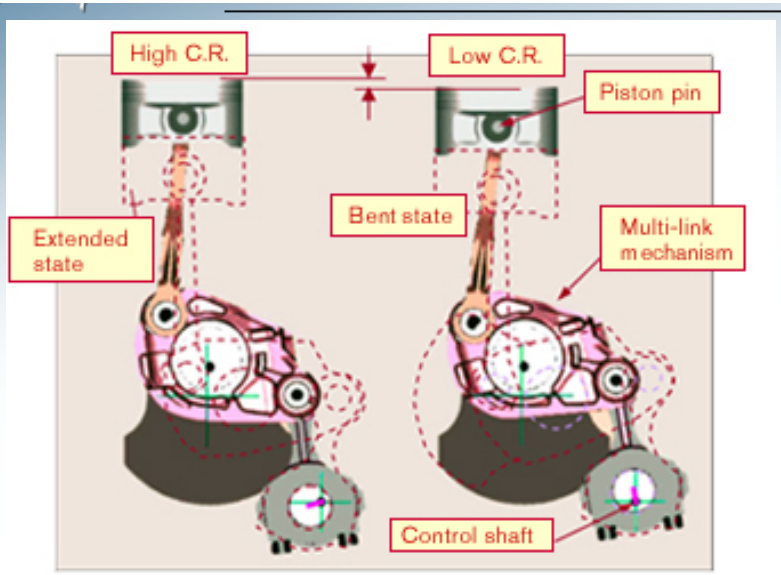

Principle of Variable Compression Ratio

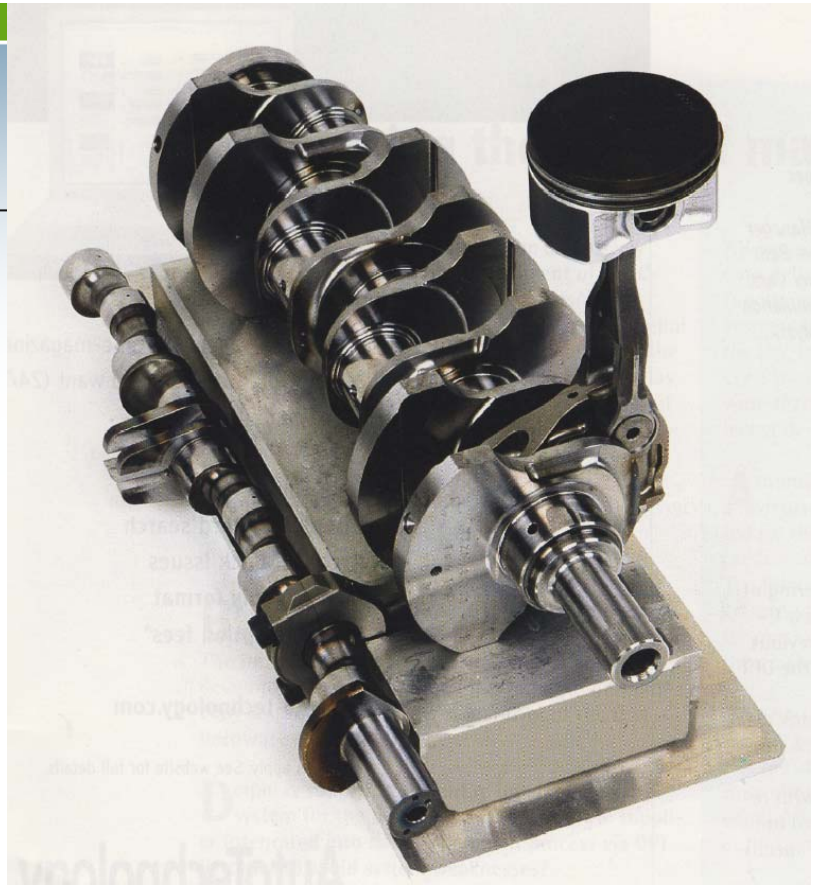

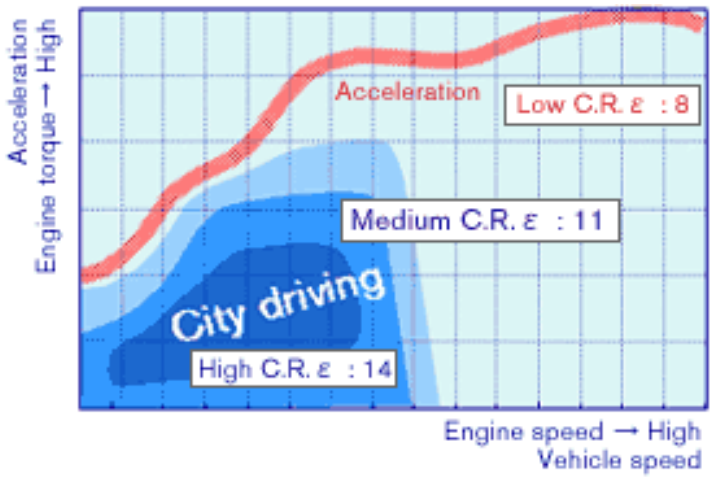

C.R. control map
(engine operating conditions)

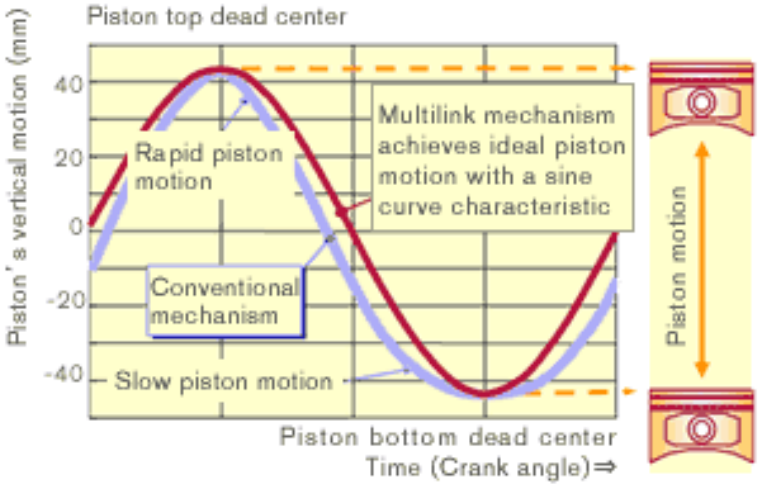

Comparison of piston strokes

Vir: NISSAN

Podaljšana ekspanzija – Atkinsonov cikel

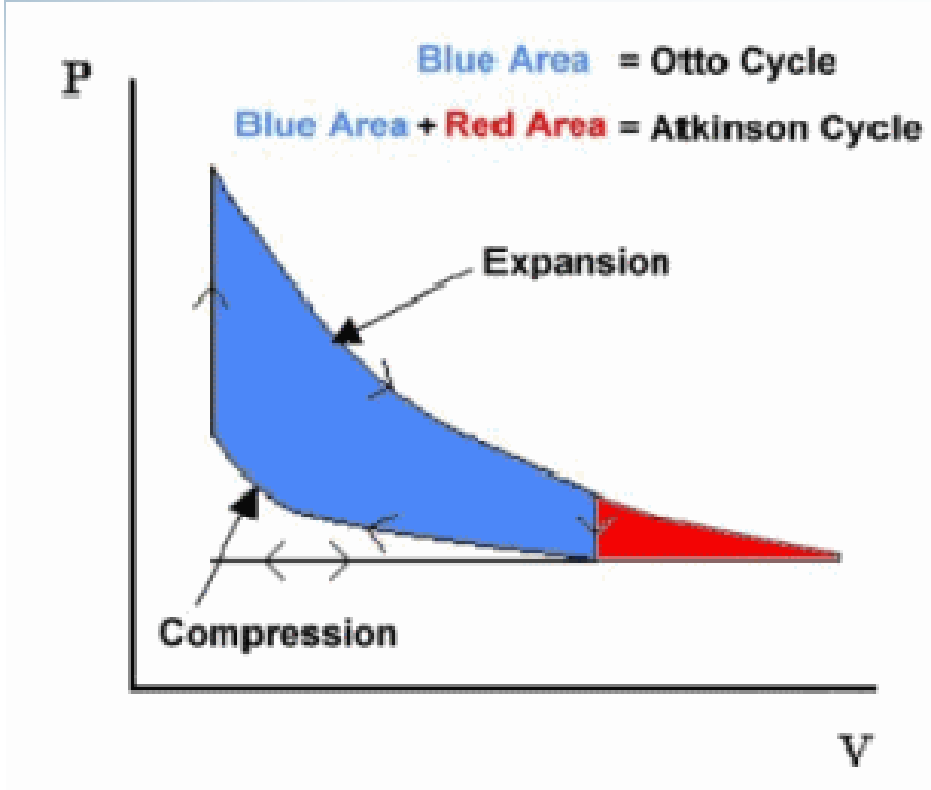

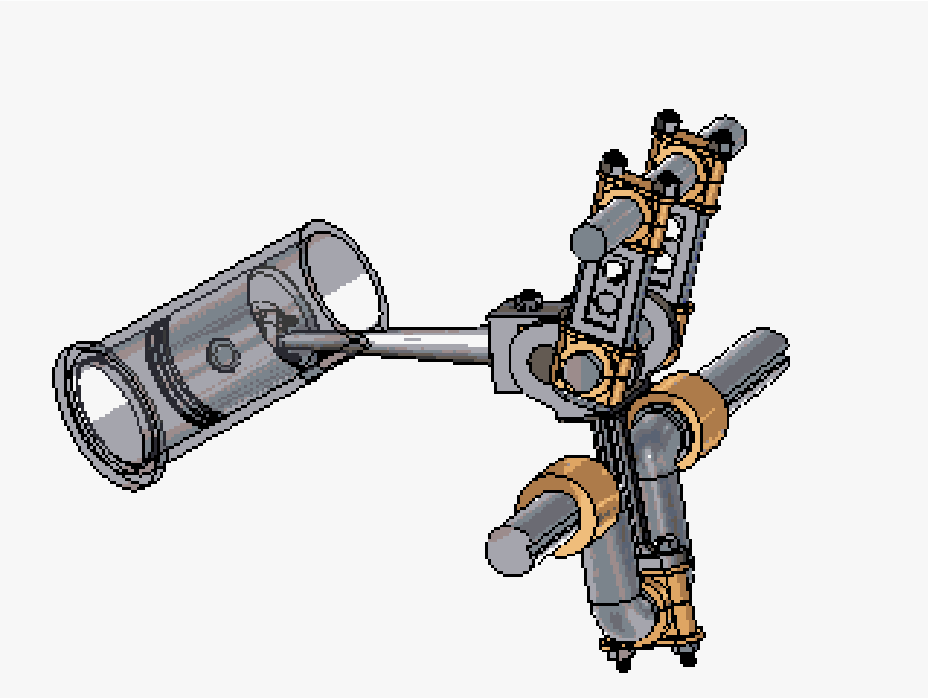

http://www.libralato.co.uk/images/fig6.gif

http://www.dself.dsl.pipex.com/MUSEUM/POWER/unusualICeng/atkinson/atkinson.htm

Podaljšana ekspanzija - Atkinsonov cikel

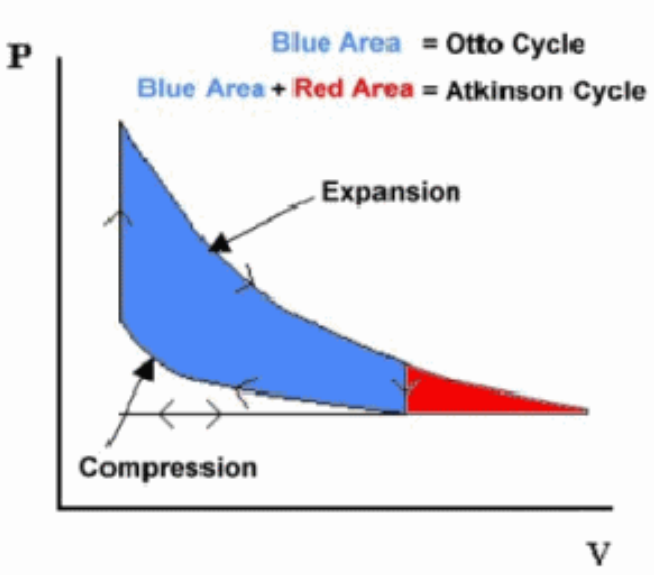

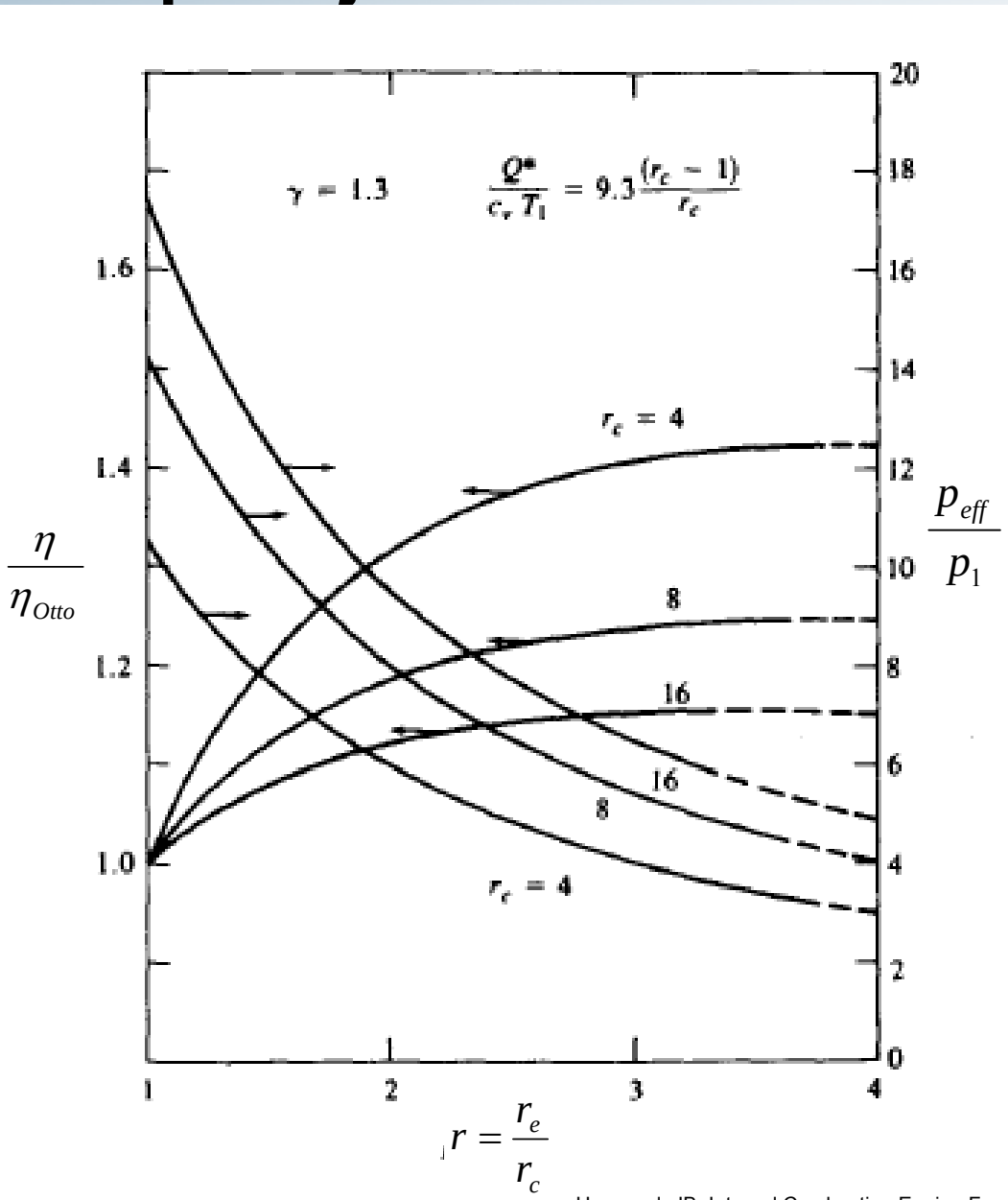

http://www.libralato.co.uk/images/fig6.gif

Heywood, JB, Internal Combustion Engine Fundamentals

Podaljšana ekspanzija – krmiljenje ventilov -> Millerjev cikel

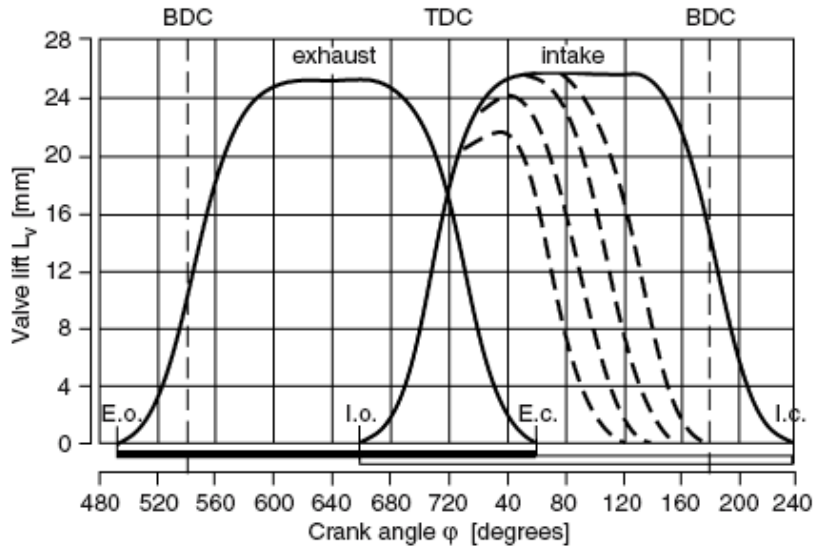

Fig. 6.19. Intake valve timing diagram for the Miller process

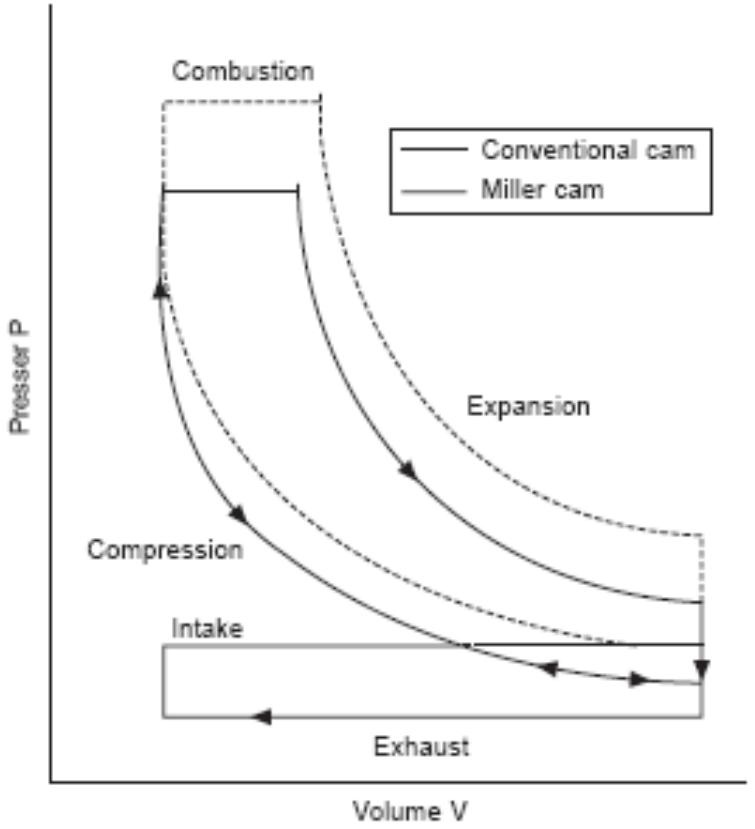

Figure 30.27 P-V diagram for Miller system (Niigata)

Hiereth H., Prenninger P., Charging the Internal Combustion Engine (Powertrain), 2007

Izmenjava delovnega medija Ottovega motorja

6 valjni motor @ 2000 1/min

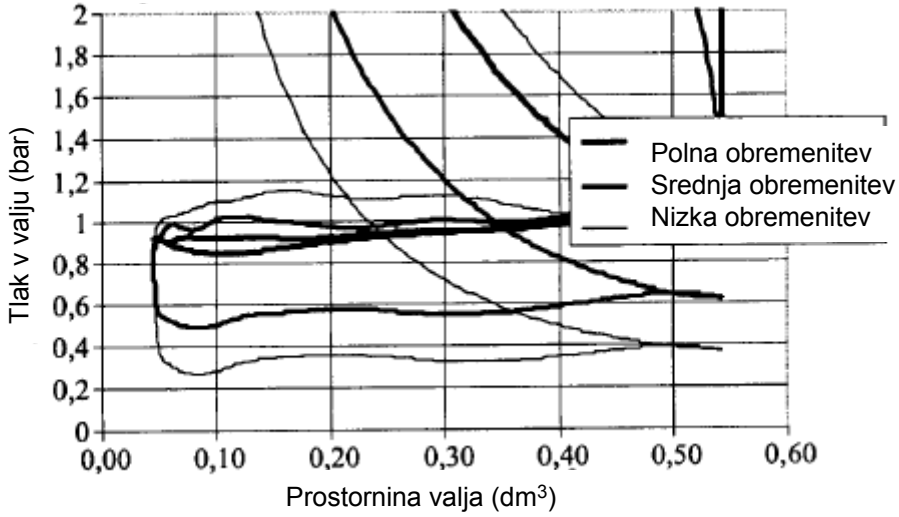

6 valjni motor @ 2000 1/min nizka obremenitev

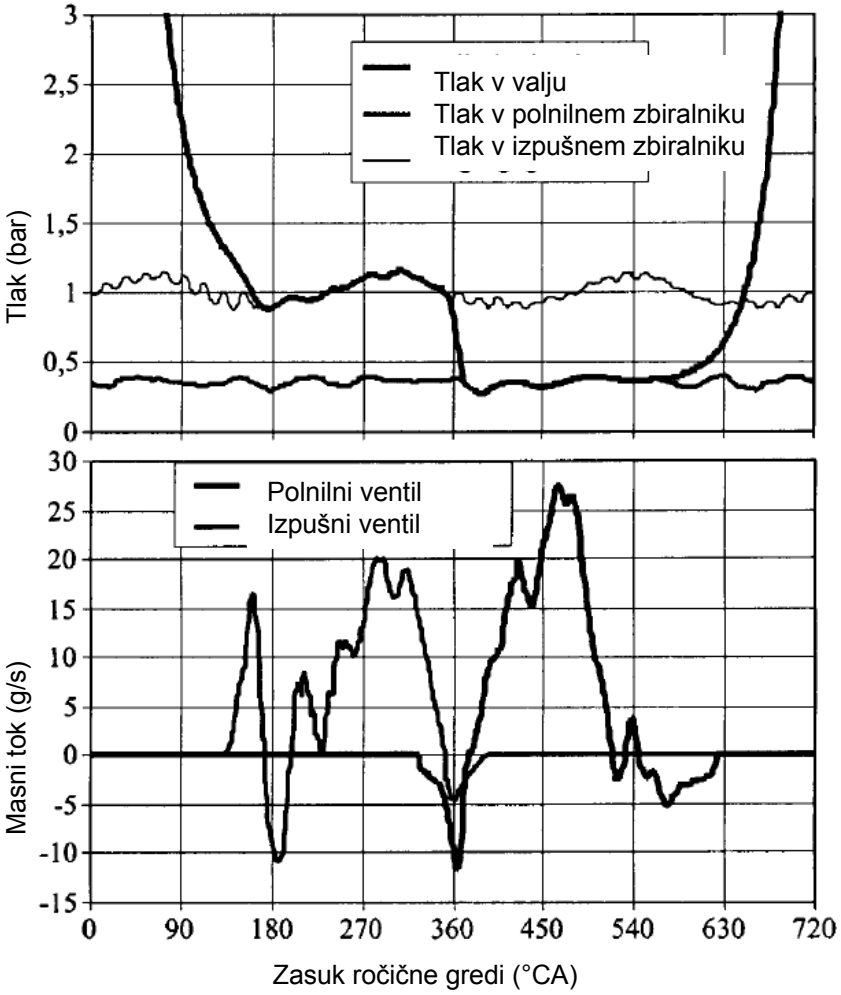

Hod ventilov in pretočna števila

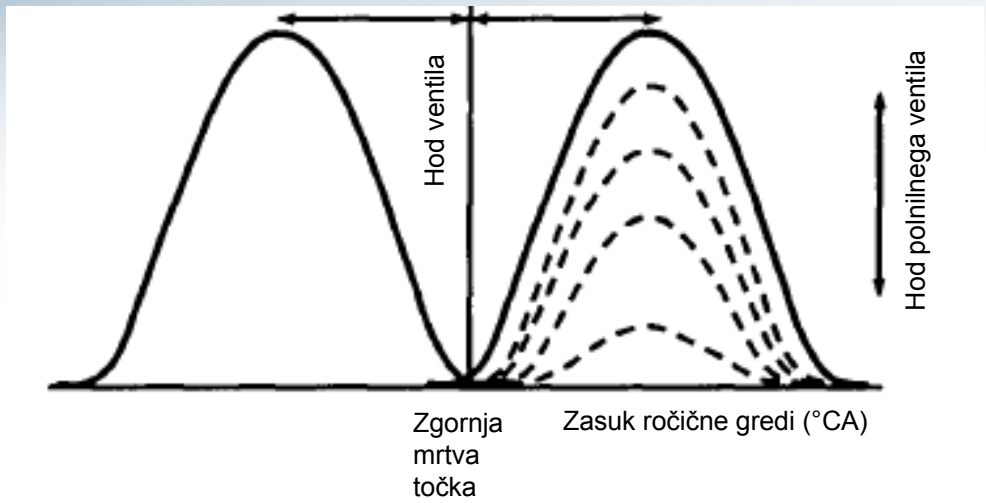

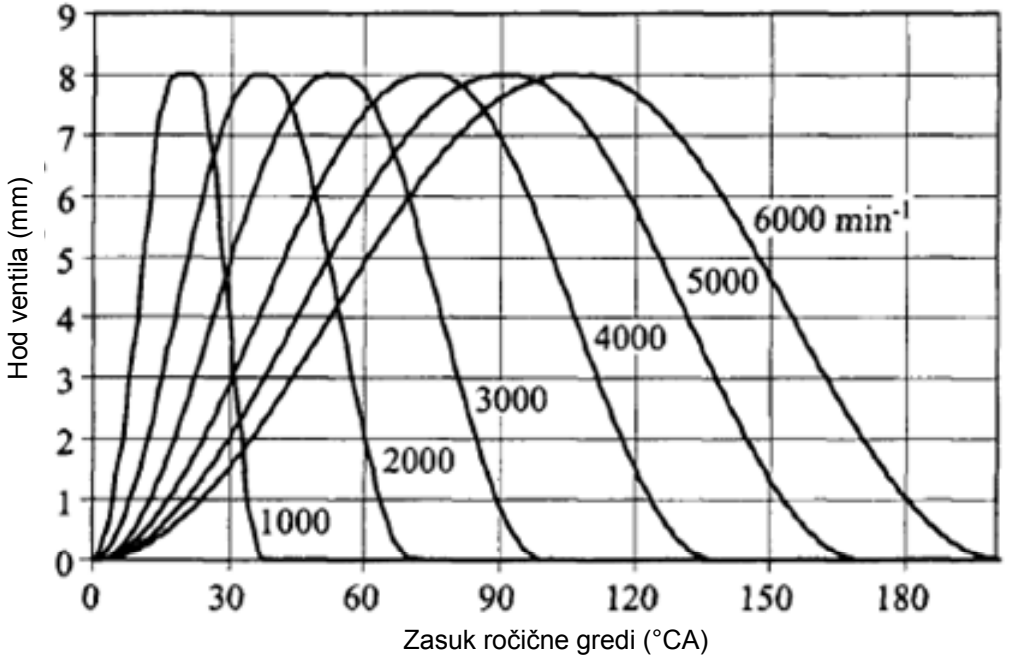

Merker GP et al, Technische Verbrennung, 2001

Vpliv krmiljenja ventilov

6 valjni motor @ 2000 1/min

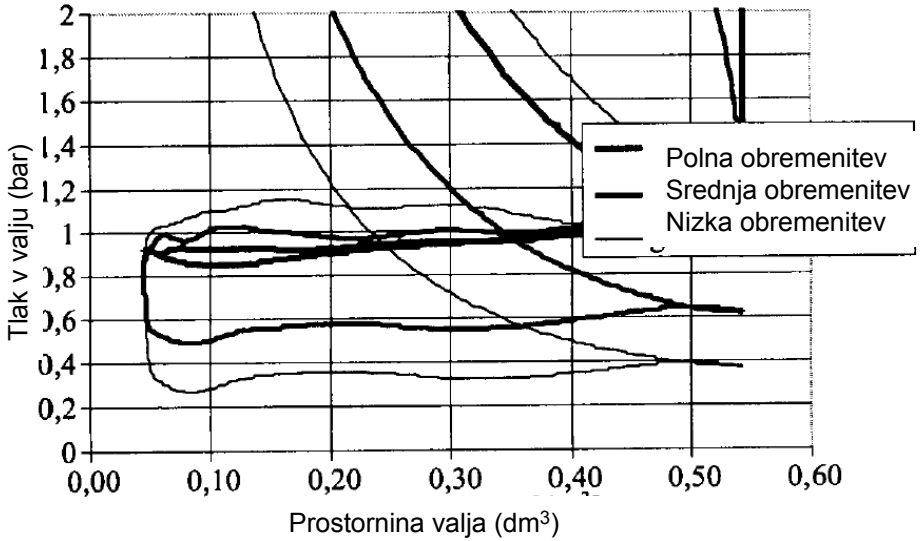

6 valjni motor @ 2000 1/min nizka obremenitev

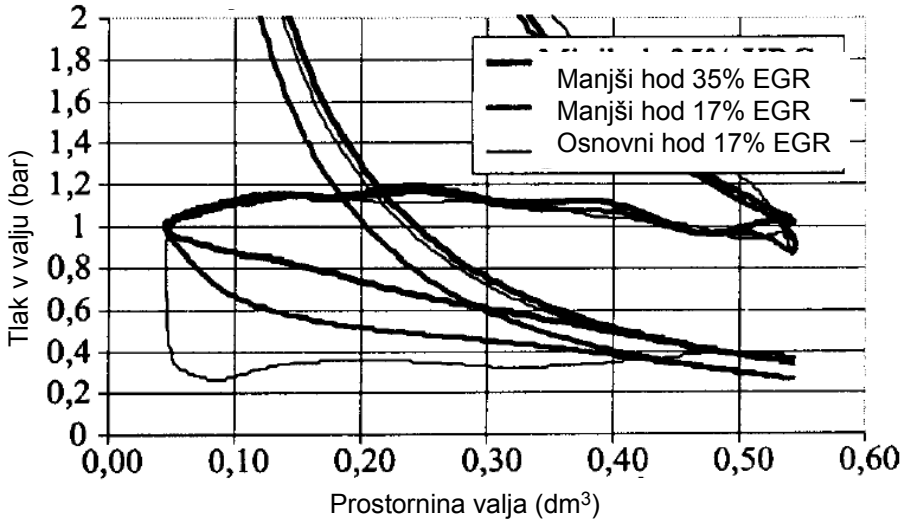

6 valjni motor @ 2000 1/min nizka obremenitev

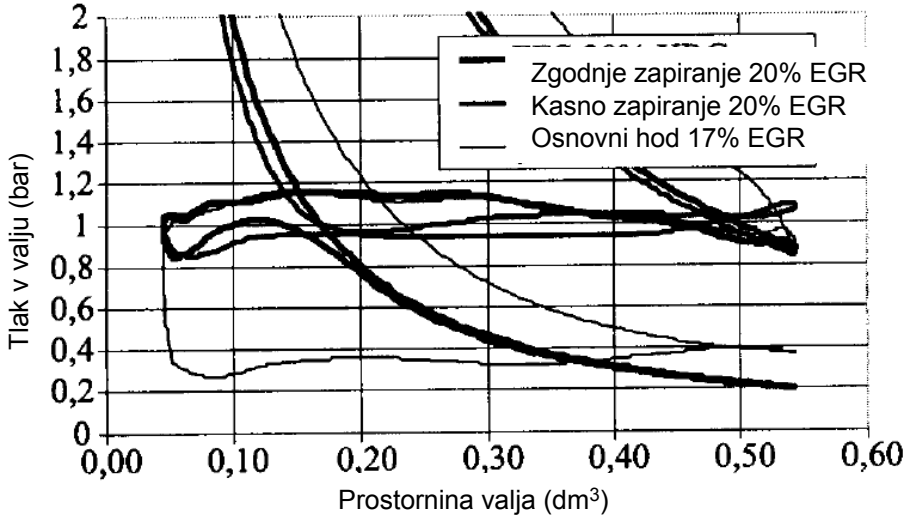

Merker GP et al, Technische Verbrennung, 2001

Izvedbe z različnim številom ventilov

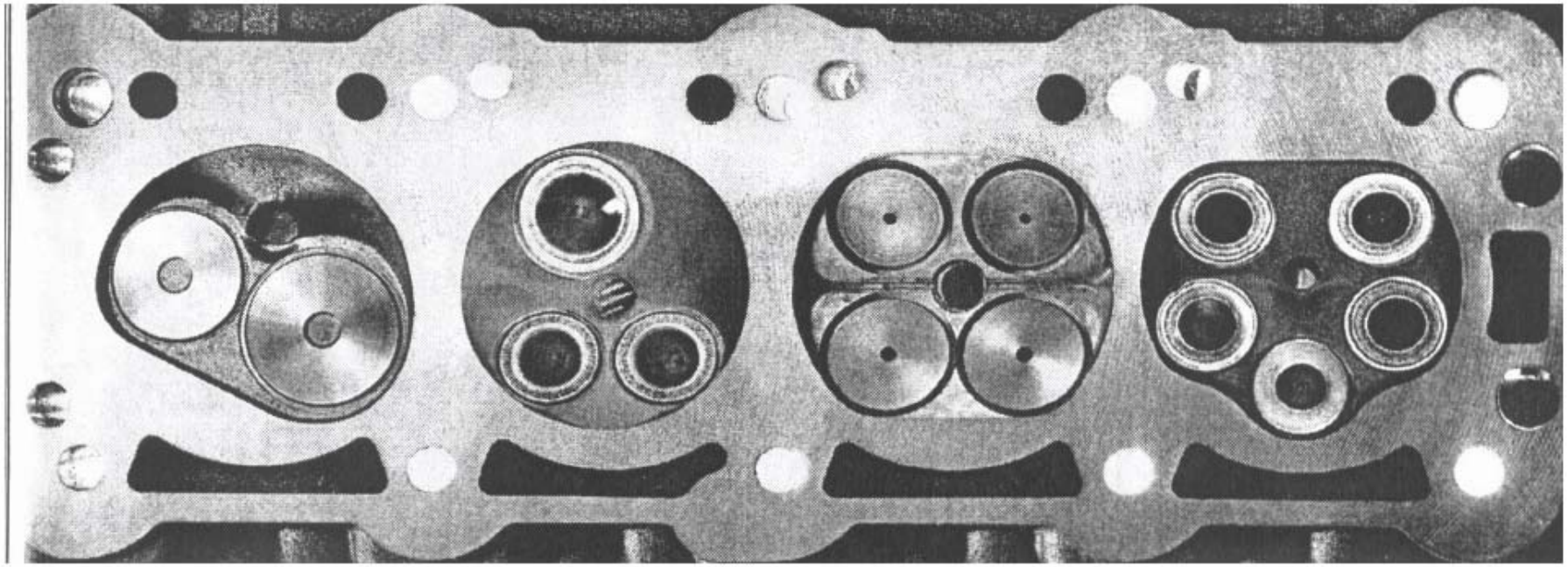

Variacija faze ventilov: BMW VANOS

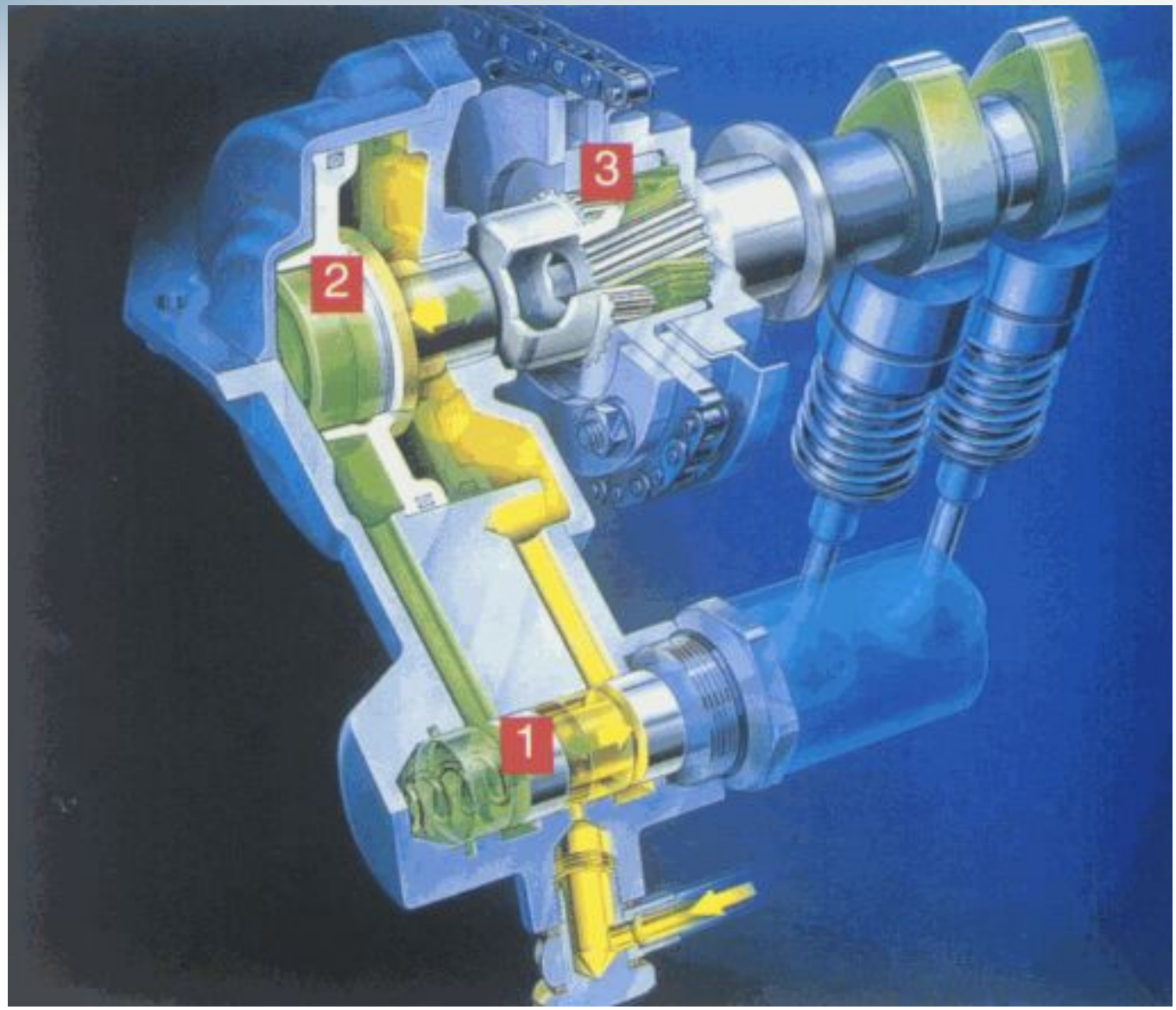

Vir: BMW

BMW Valvetronic

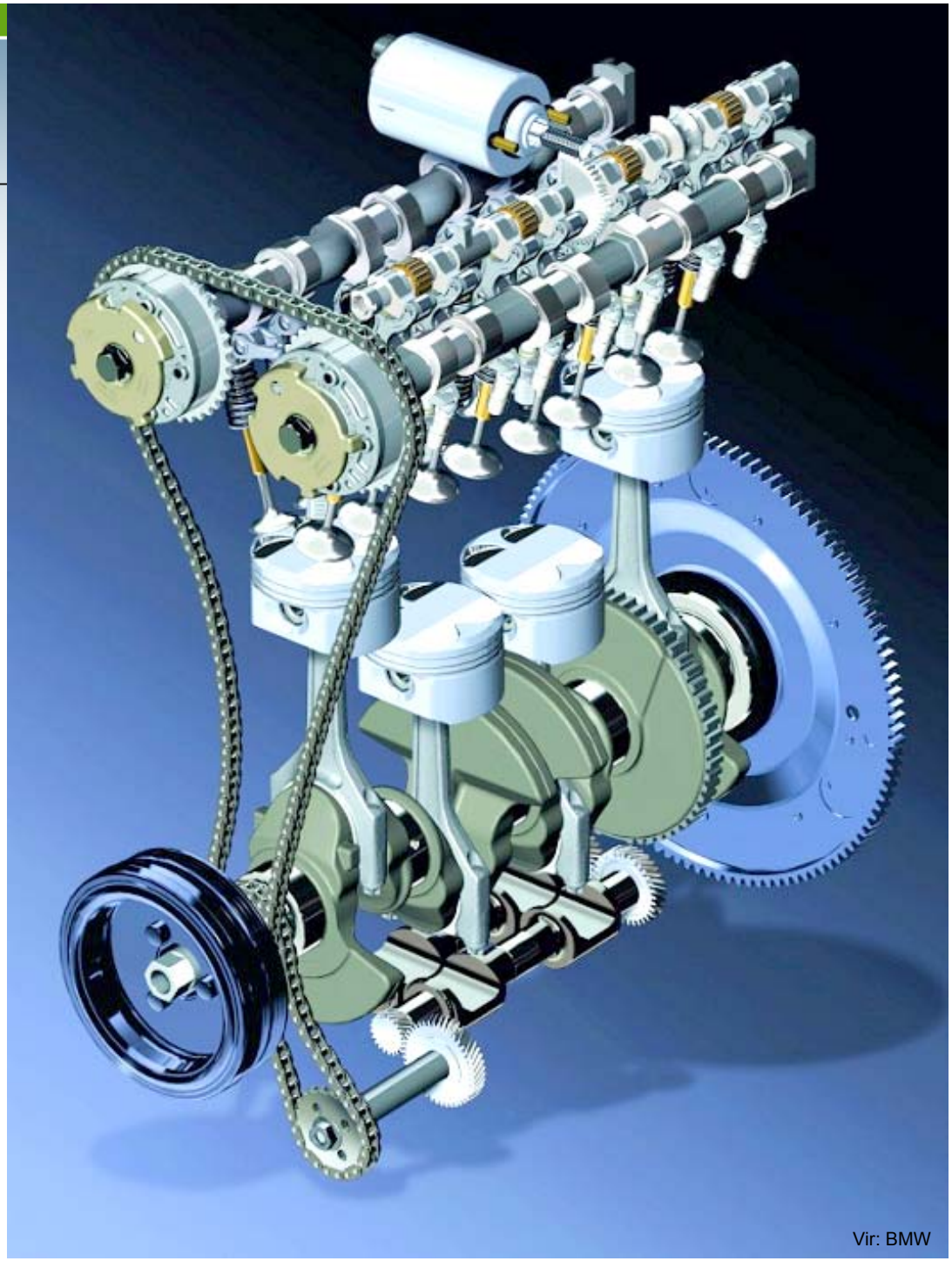

Vir: BMW

BMW Valvetronic

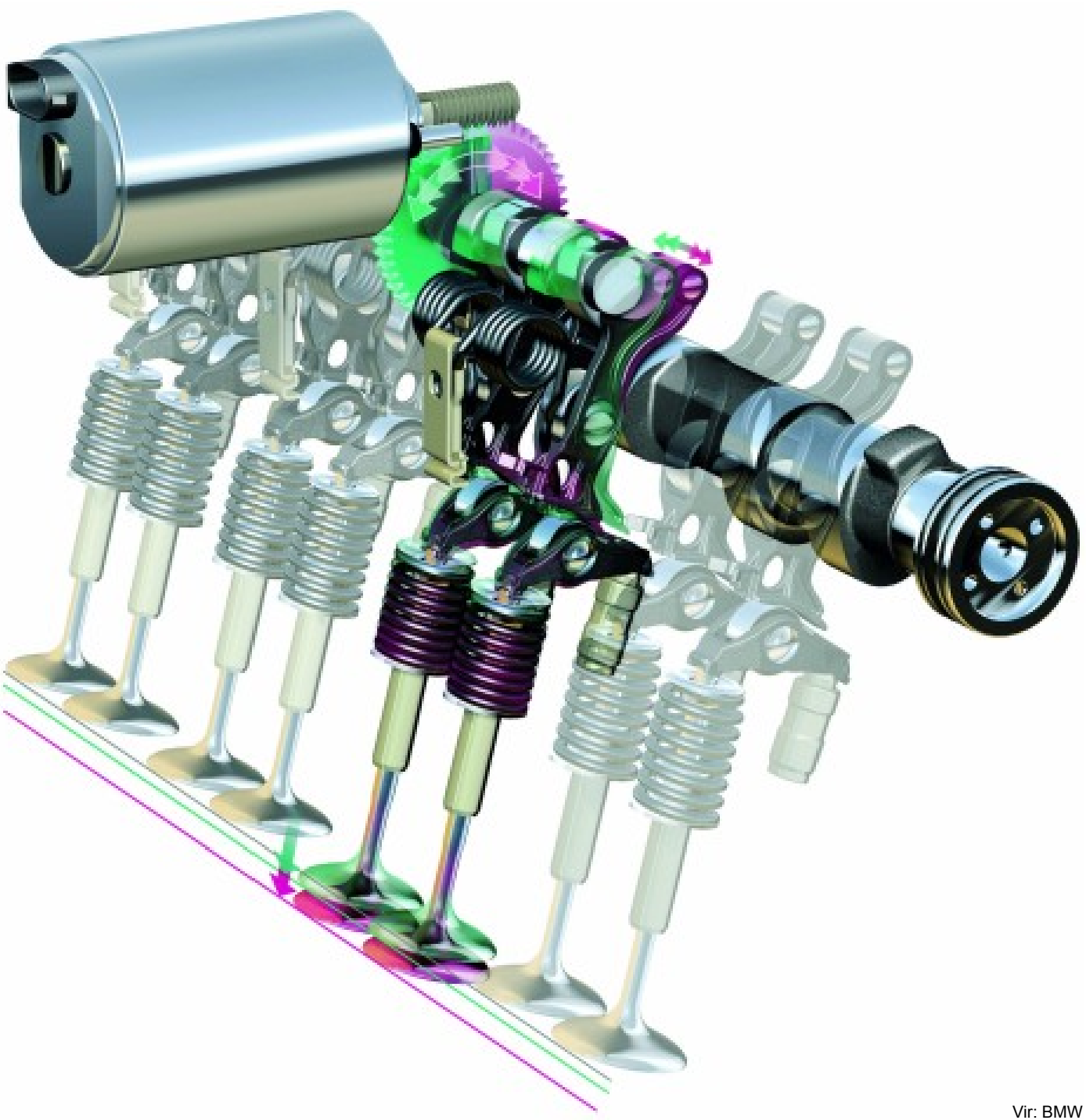

Vir: BMW

Elektro-hidravlično krmiljenje ventilov

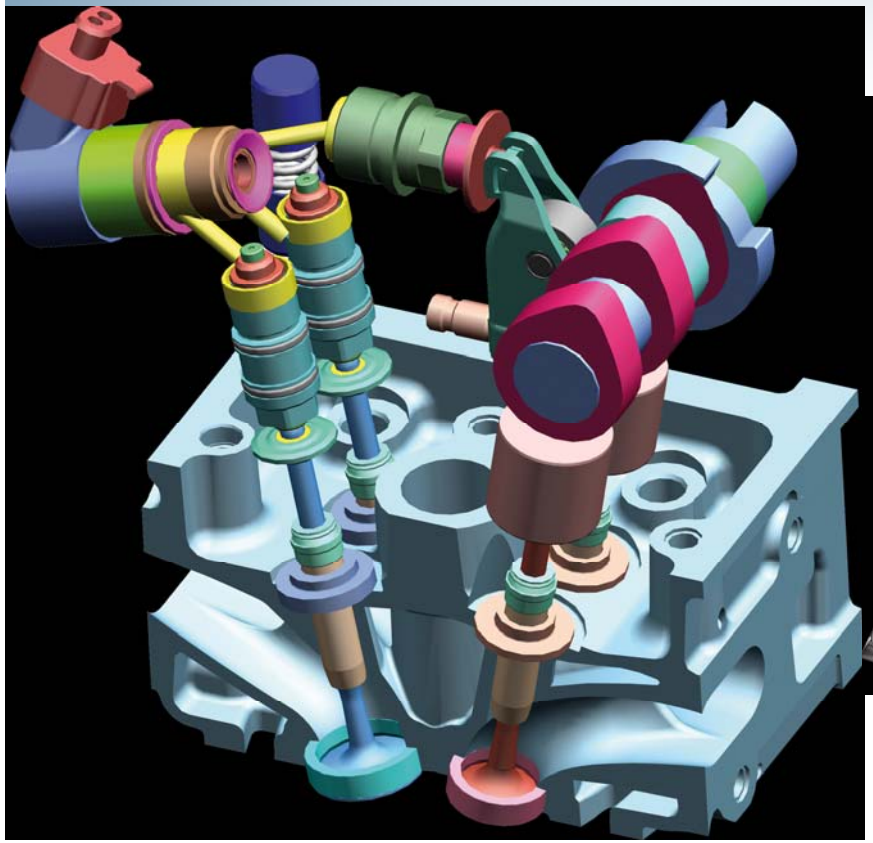

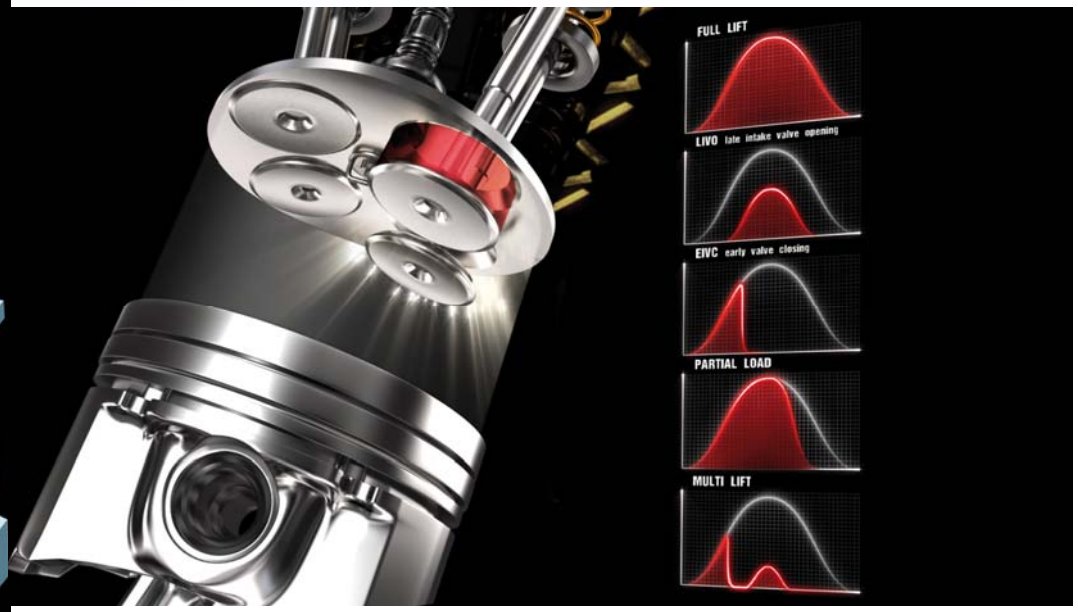

http://www.greencarcongress.com/2009/03/fiat-introduces.html

Elektro-hidravlično krmiljenje ventilov

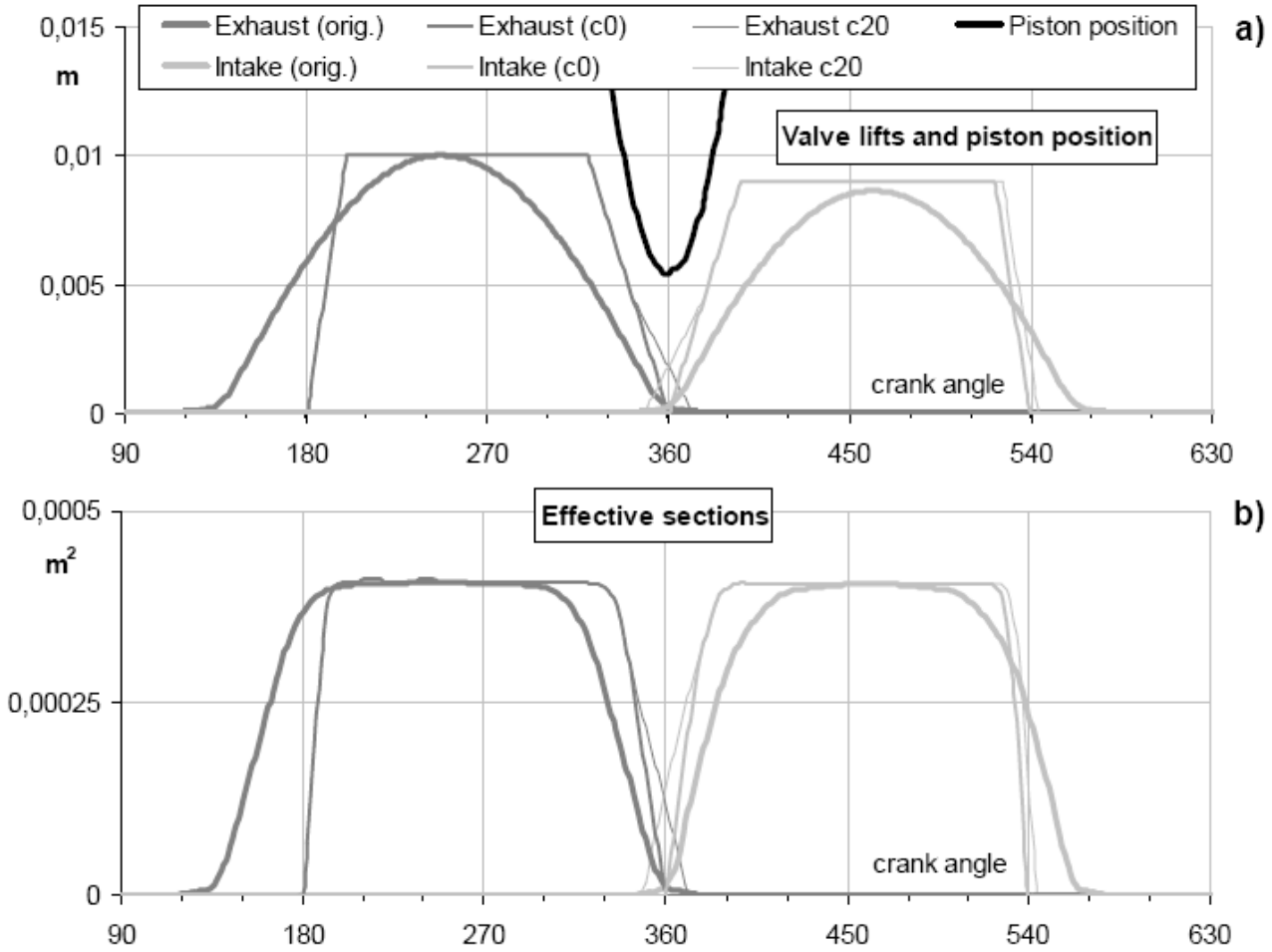

Figure 3. Valve lifts and effective sections generated by original and camless valve actuation systems.

Elektro-hidravlično krmiljenje ventilov

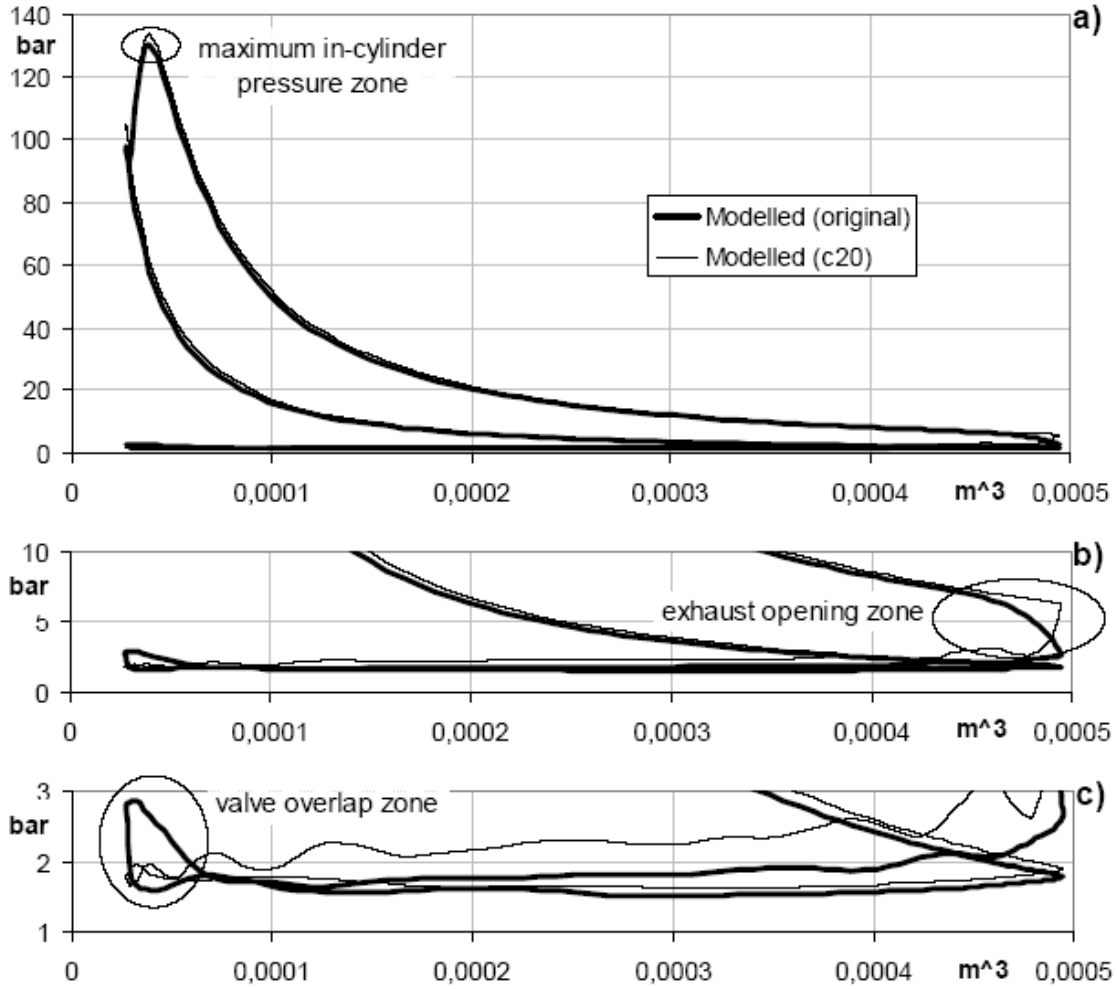

Figure 9. P-V diagram at the end of the 1500 rpm load transient for original valve lifts and c20 valve lifts.

Elektro-hidravlično krmiljenje ventilov

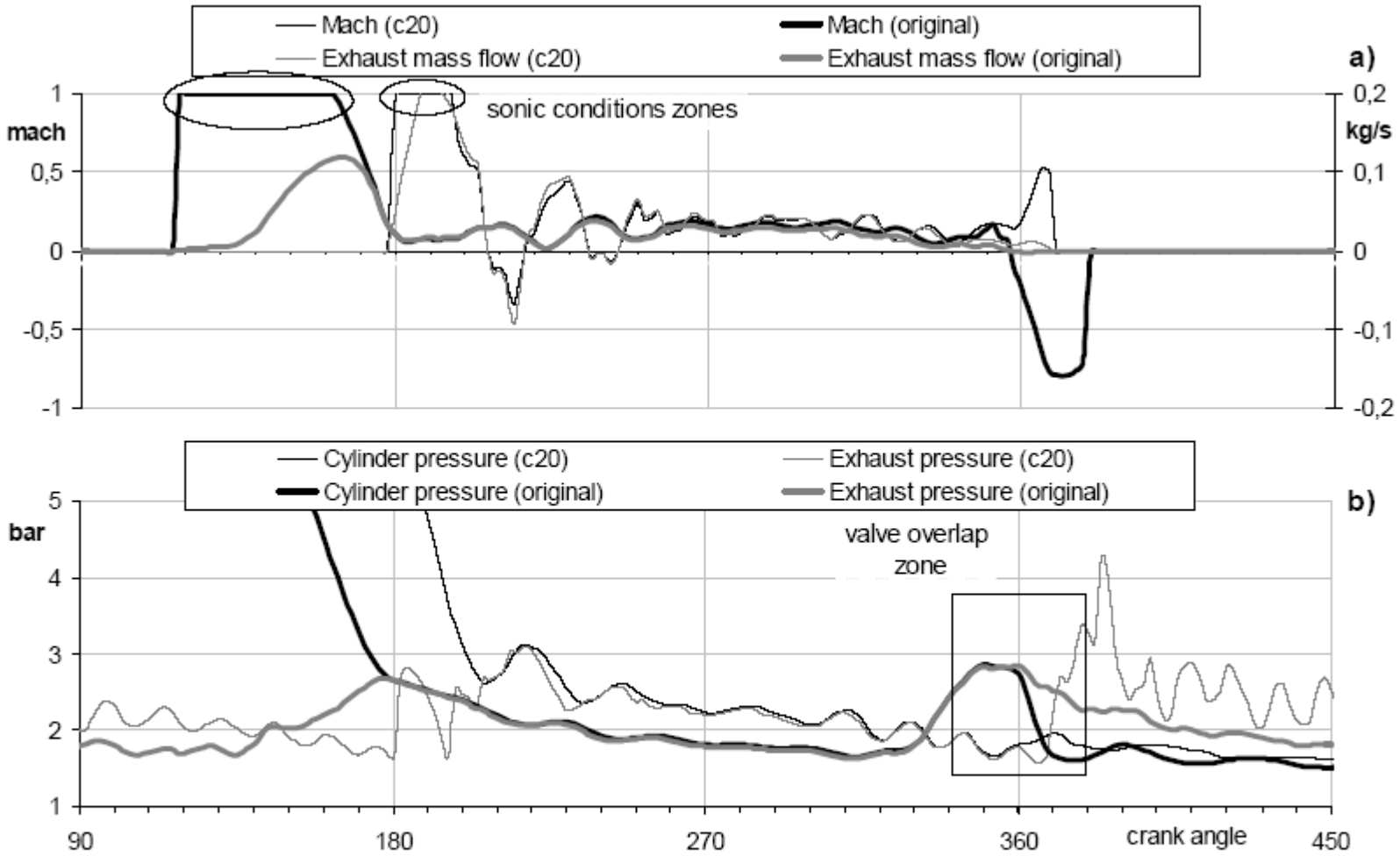

Figure 10. Pressures, Mach number and air mass flow evolutions during the exhaust period, when the 1500 rpm load transient is finishing, for original and c20 configurations.

Tlačno polnjenje

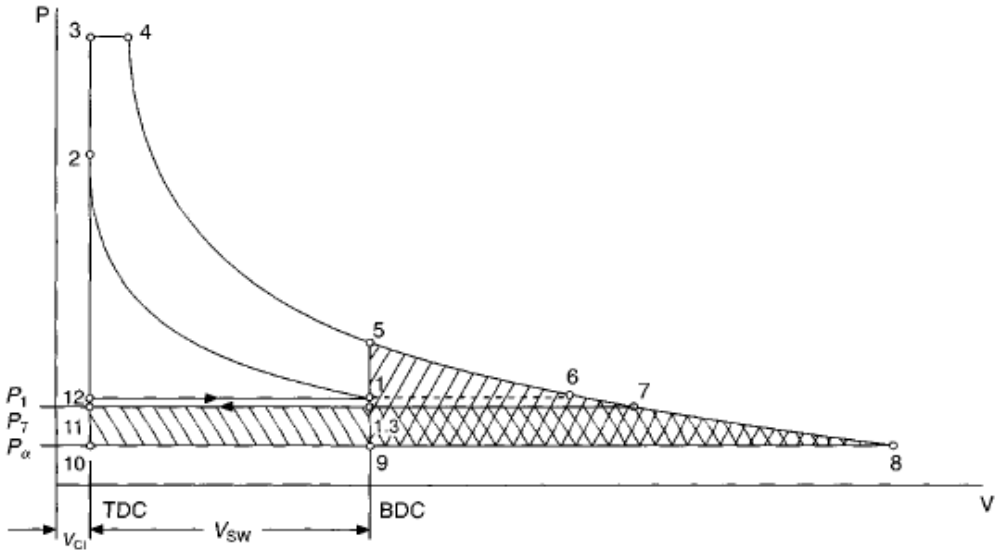

Figure 2.18 Ideal turbocharged limited pressure cycle

$$p_{eff} = \frac{p_1}{c_v T_1} \frac{m_f H_{LHV}}{m} \frac{\varepsilon}{\varepsilon - 1} \frac{1}{\kappa - 1} \eta$$

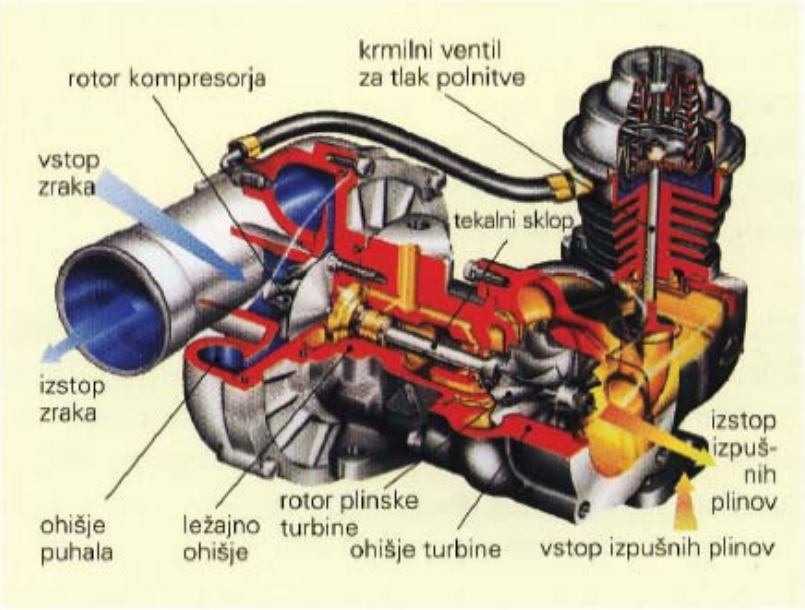

Slika 2.5.2-1: Sestavni deli tlačnega polnilnika na izpušne pline

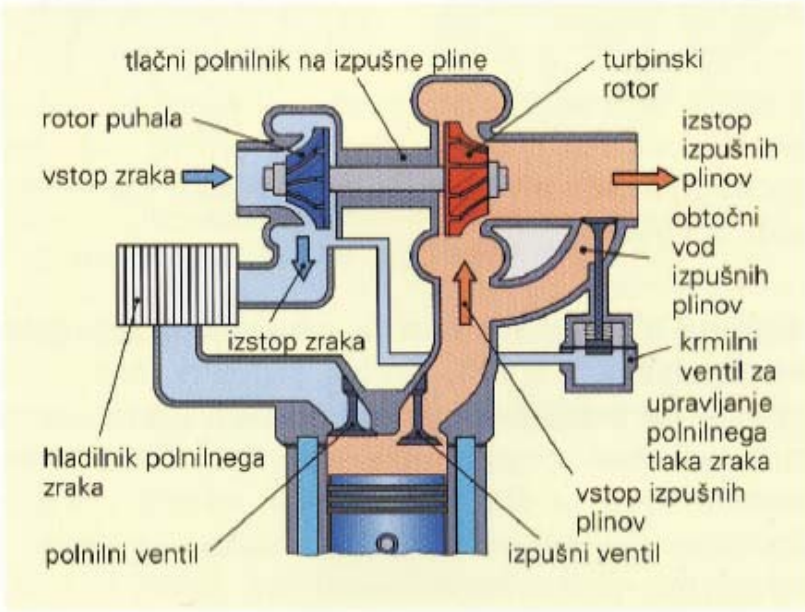

Slika 2.5.2-2: Shema motorja s tlačnim polnilnikom na izpušne pline

Vir: Motorno vozilo, 2004

Tlačno polnjenje

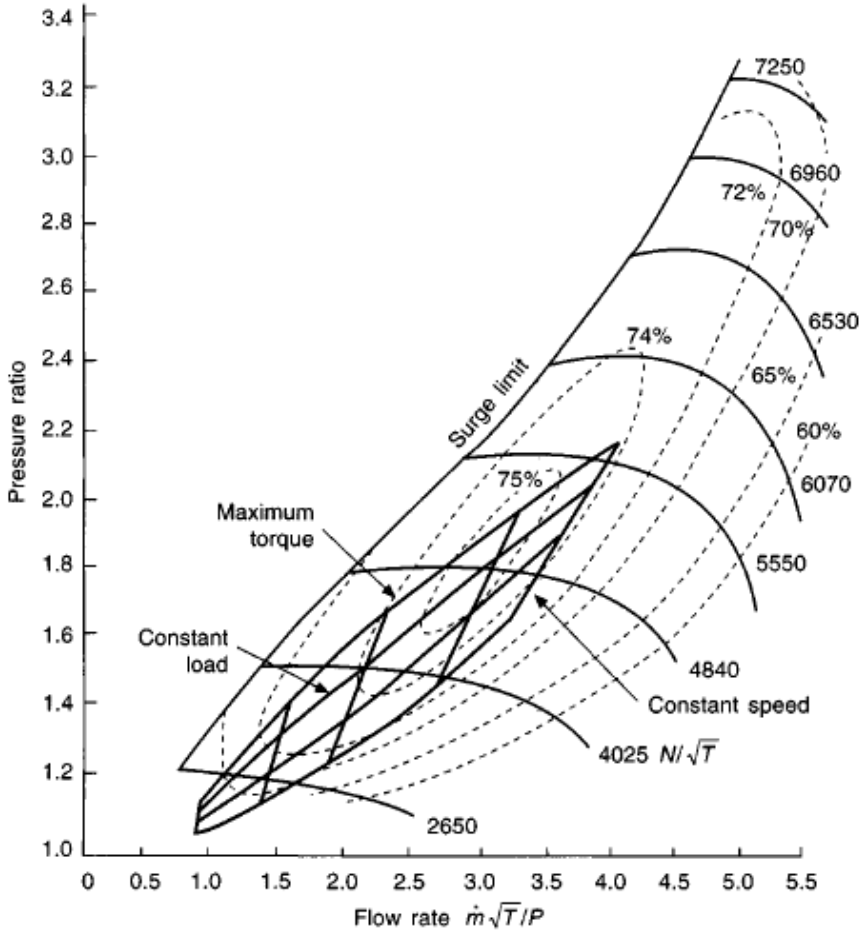

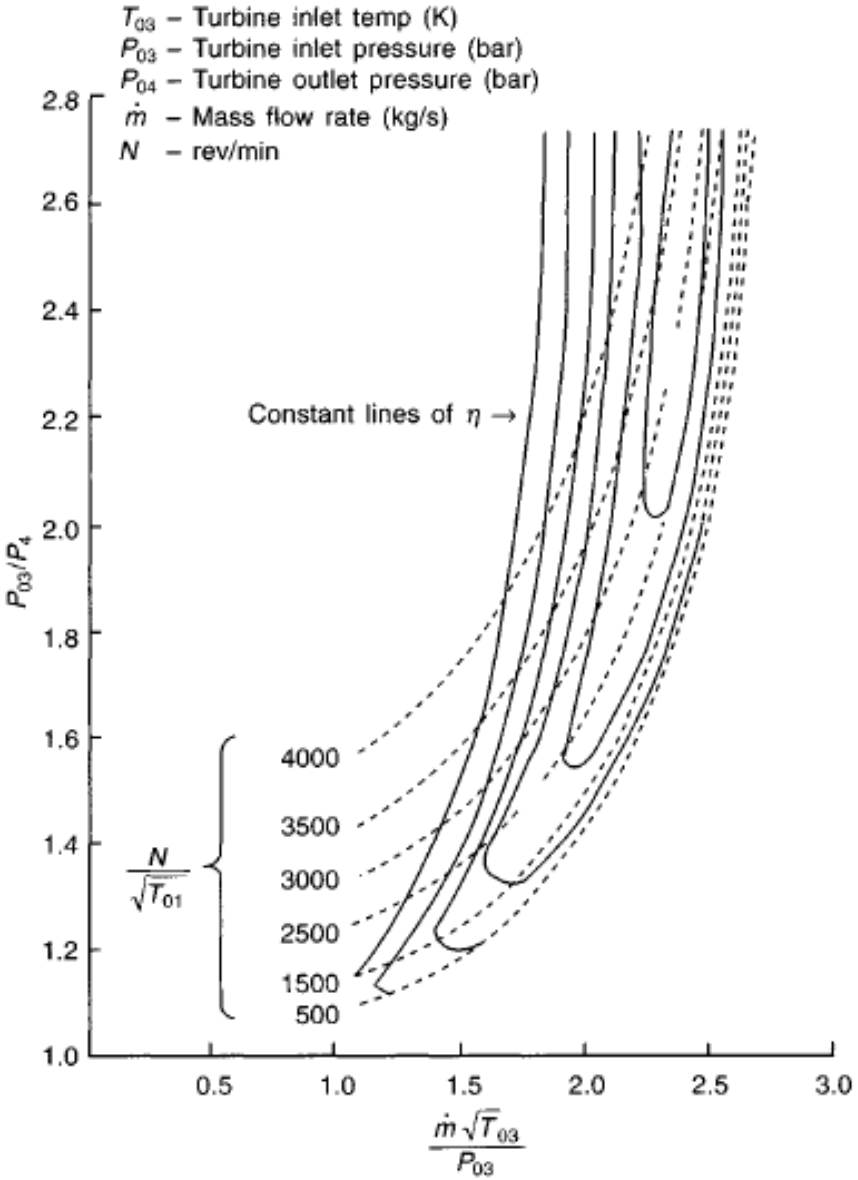

Figure 2.14 Radial flow turbine performance map

Figure 2.58 Engine operating area superimposed on compressor map, showing surge margin with reduced turbine area

Challen B, Baranescu R, Diesel engine Reference book

Spremenljiva geometrija vodilnih lopatic plinske turbine

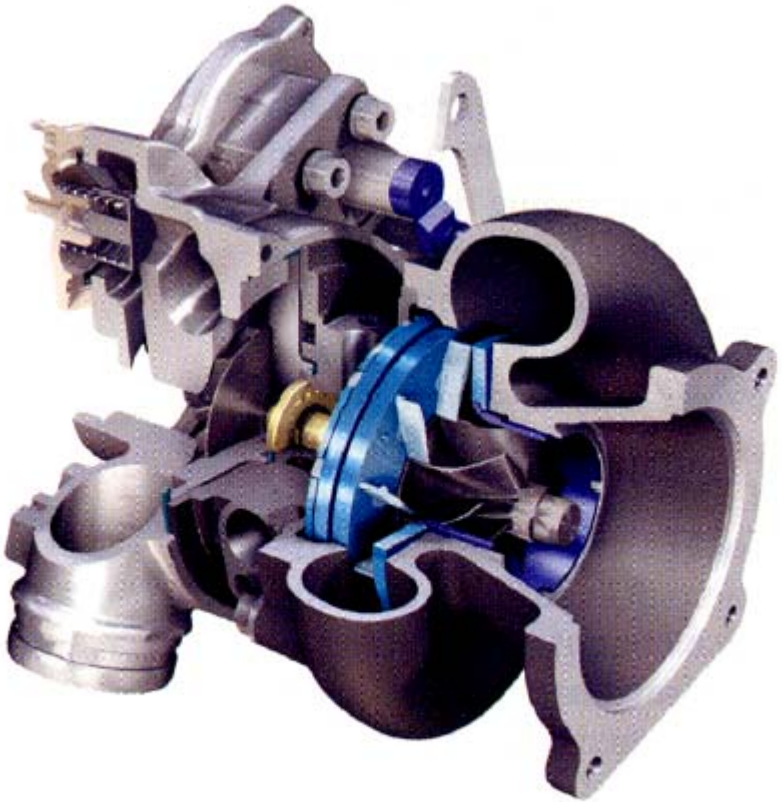

Figure 6: Turbocharger with variable turbine geometry.

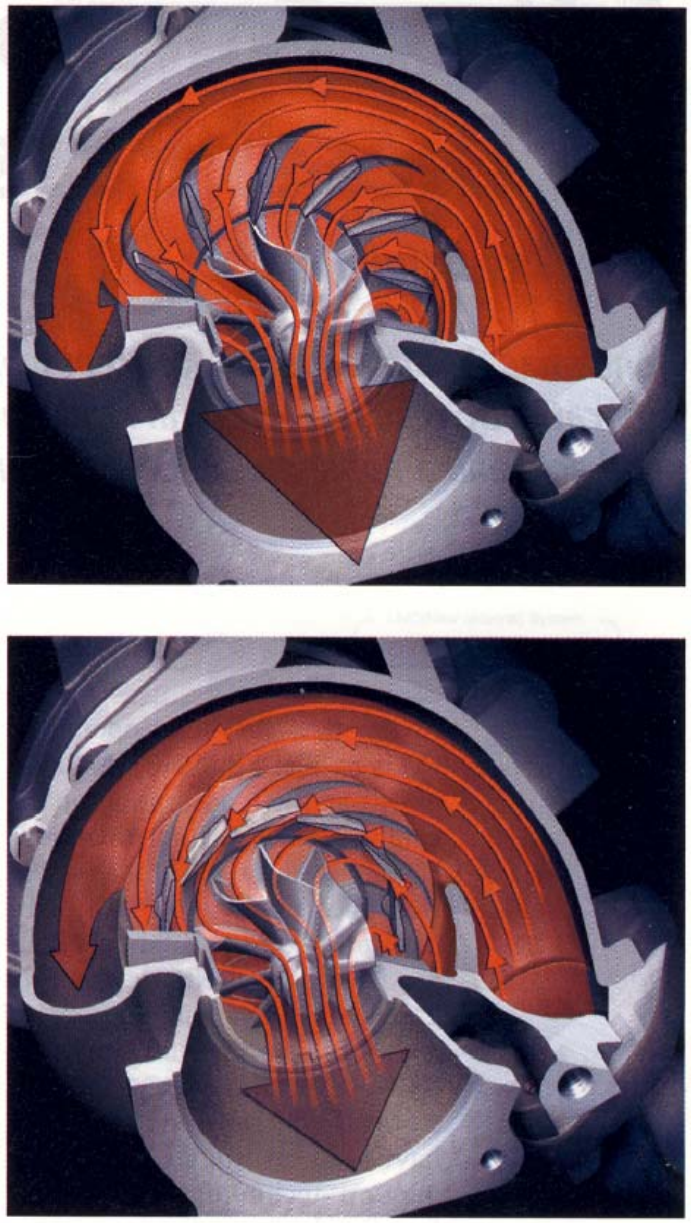

Figure 7: Operating principle of variable turbine geometry. 7a: Vanes closed, small turbine; 7b: Vanes open, large turbine.

Vir: ATZ

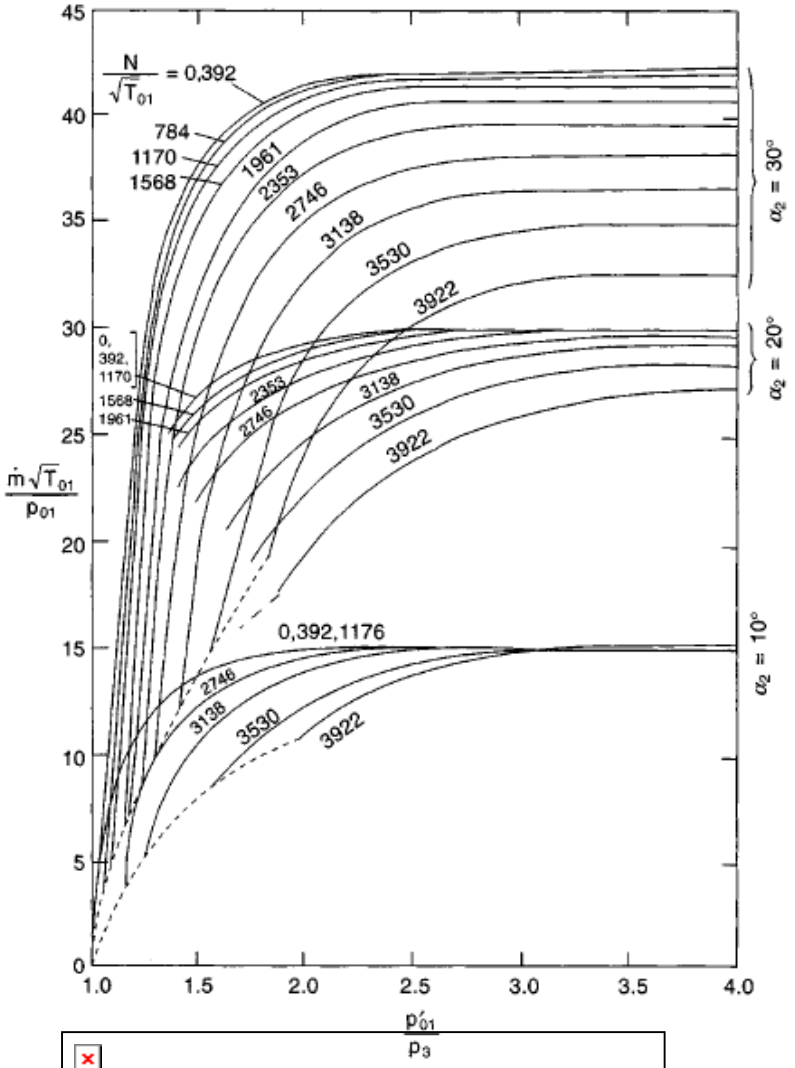

Challen B, Baranescu R, Diesel engine Reference book

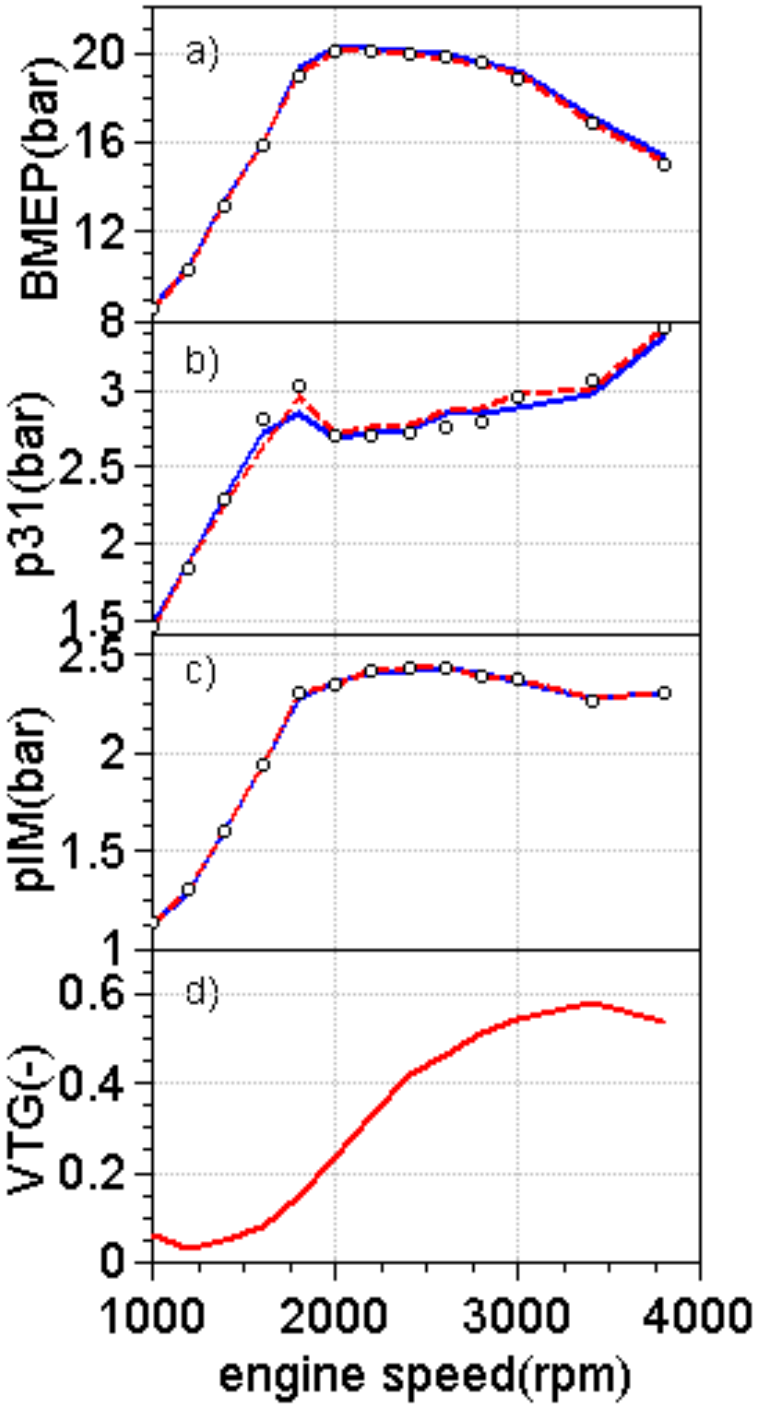

Večstopenjsko tlačno polnjenje

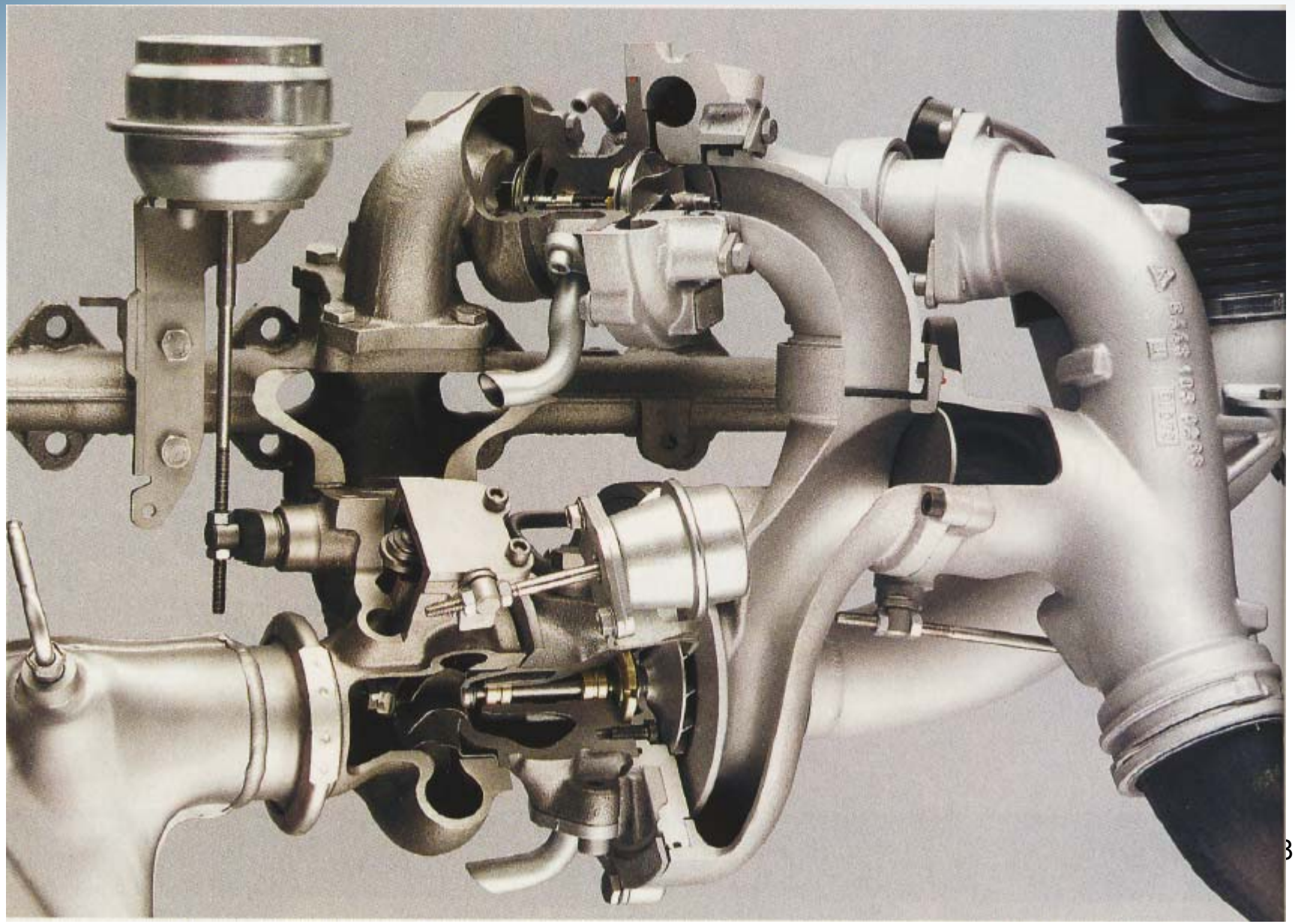

Vir: ATZ

Večstopenjsko tlačno polnjenje

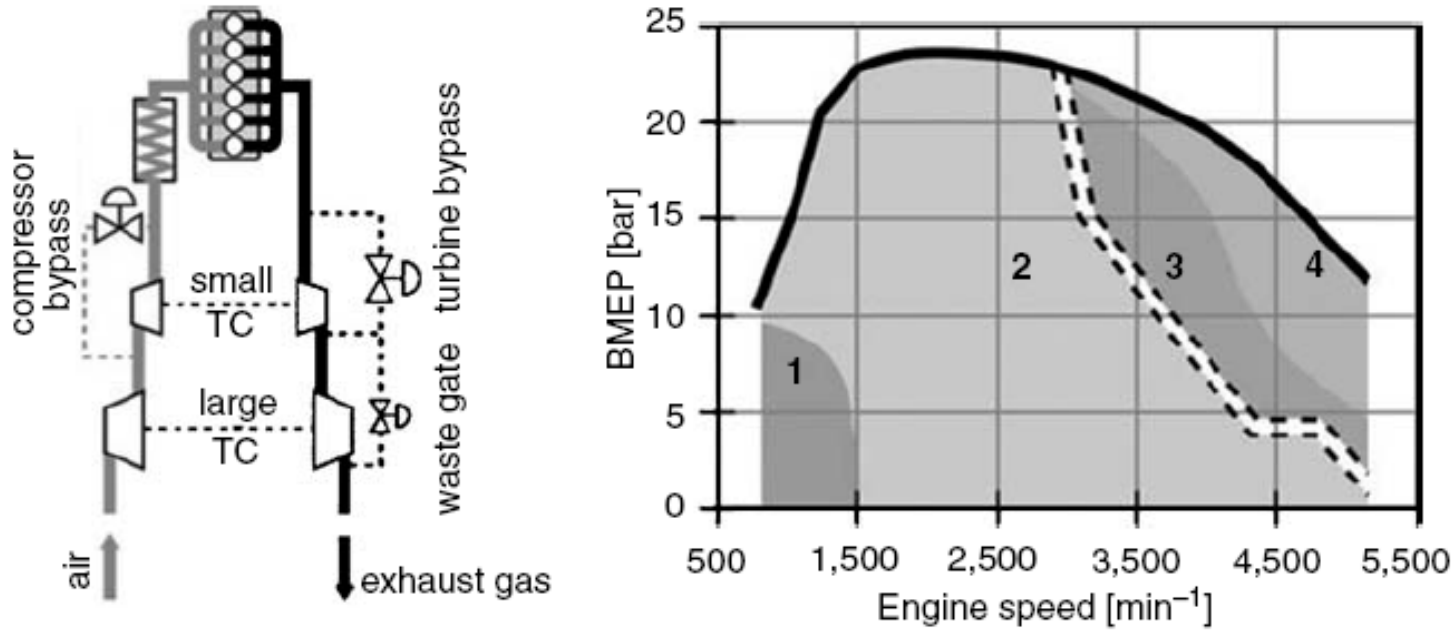

Fig. 14.41. Sketch of turbocharging system and operating strategy of the BMW 3 liter, 6-cylinder DI diesel engine with mixed two-stage and register turbocharging [133]. Operating range 1: turbine bypass closed, compressor bypass closed, waste gate closed. Operating range 2: turbine bypass controlled opened, compressor bypass closed, waste gate closed. Operating range 3: turbine bypass open, compressor bypass open, waste gate closed. Operating range 4: turbine bypass open, compressor bypass open, waste gate controlled opened

Hiereth H., Prenninger P., Charging the Internal Combustion Engine (Powertrain), 2007

Vmesno hlajenje polnilnega zraka

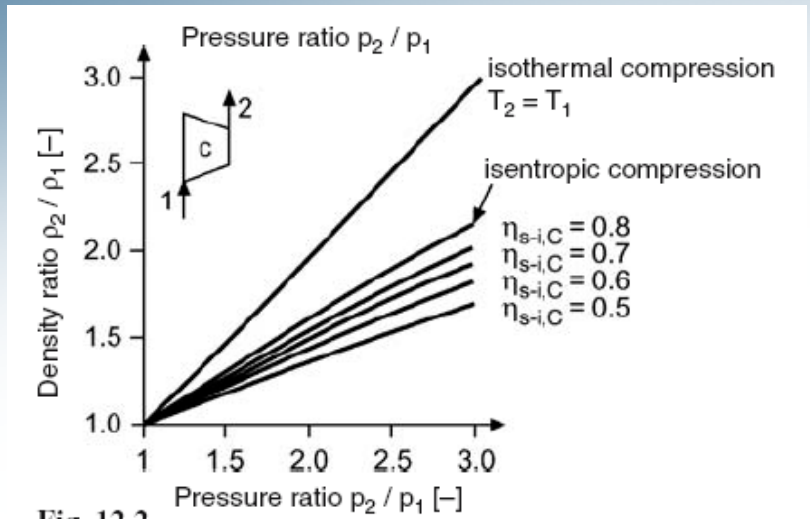

Fig. 12.2

Fig. 12.2. Charge air density increase depending on pressure ratio and compressor efficiency

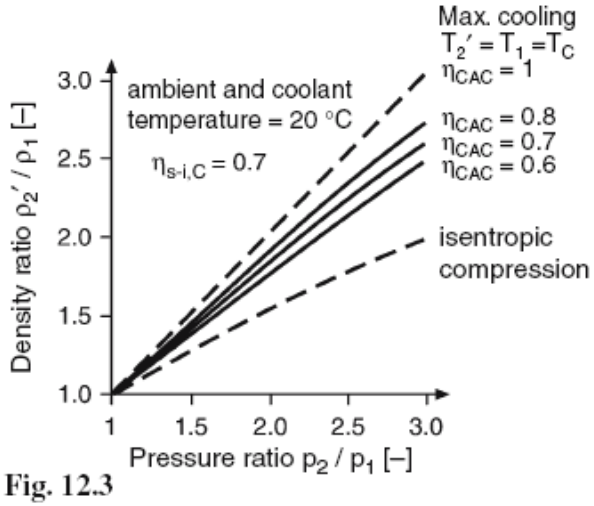

Fig. 12.3

Fig. 12.3. Charge air density status before and after cooling depending on pressure ratio and intercooler efficiency

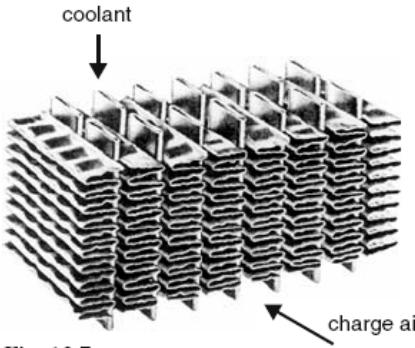

Fig. 12.7

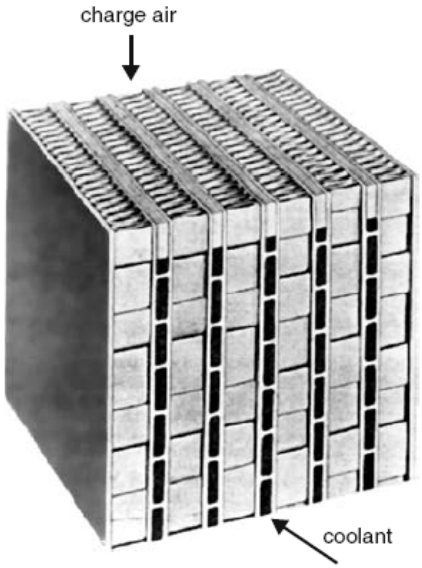

Fig. 12.8

Fig. 12.7. Flat-oval-tube lamella intercooler without interior fins [115]

Fig. 12.8. Flat-tube intercooler in rod-sheet design [115]

$$p_{eff} = \frac{p_1}{c_v T_1} \frac{m_f H_{LHV}}{m} \frac{\varepsilon}{\varepsilon - 1} \frac{1}{\kappa - 1} \eta$$

Hiereth H., Prenninger P., Charging the Internal Combustion Engine (Powertrain), 2007

Dinamična tlačna polnitev

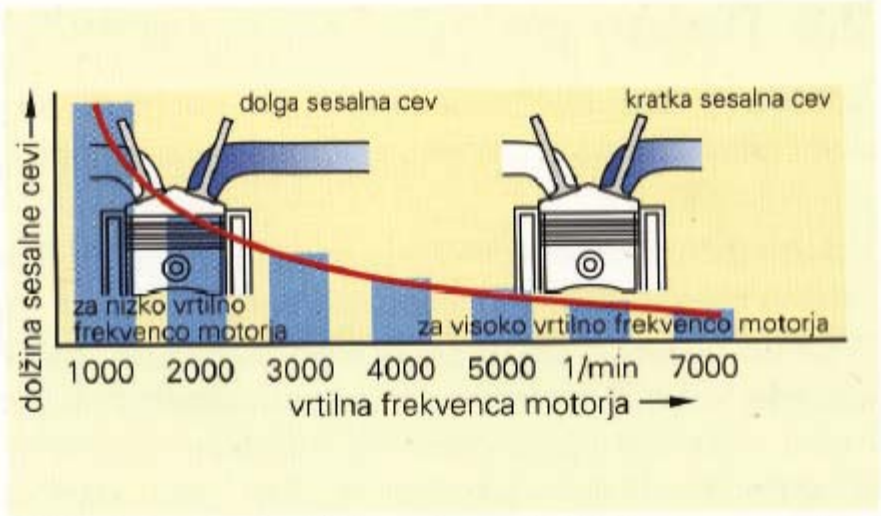

Slika 2.5.1-2: Soodvisnost med dolžino resonančne sesalne cevi in vrtilno frekvenco motorja

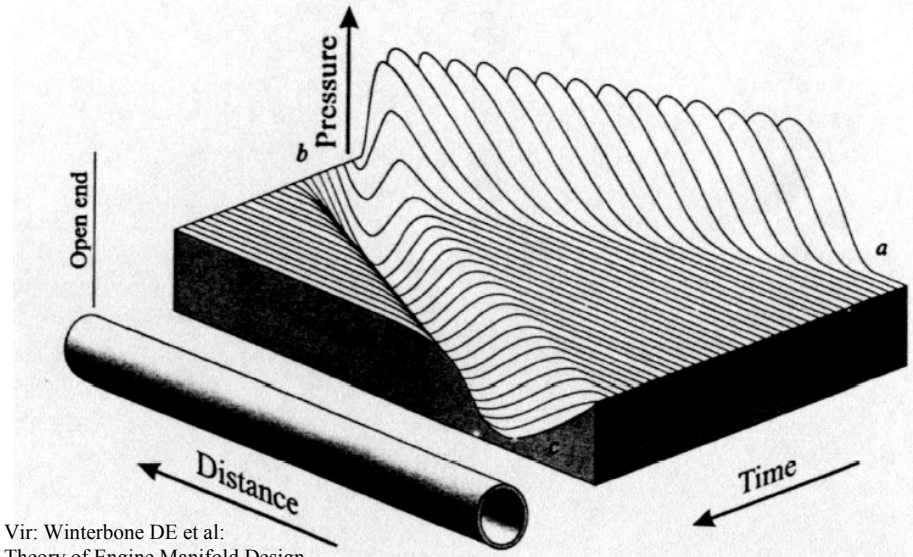

Vir: Winterbone DE et al: Theory of Engine Manifold Design, PE Publishing 2000

Odboj tlačnega vala na odprtem koncu

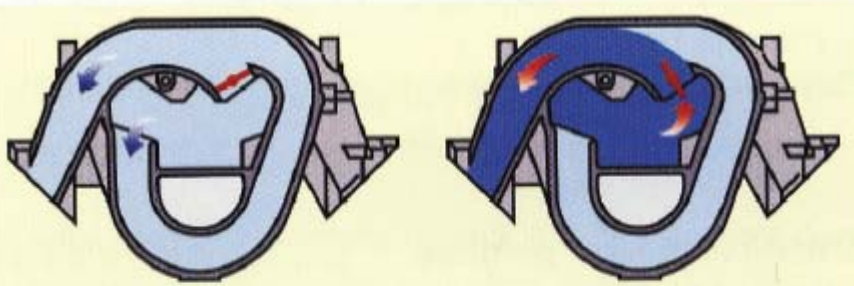

Dolga sesalna cev z zaprto preklopno loputo ustreza uglasitvi motorja na vrtilne frekvence motorja pod 4100 vrt/min.

Kratka sesalna cev z odprto preklopno loputo je primerna za uglasitev vstopnega sistema motorja na vrtilne frekvence motorja nad 4100 vrt/min.

Slika 2.5.1-3: Sesalni sistem z različnimi sesalnimi cevmi

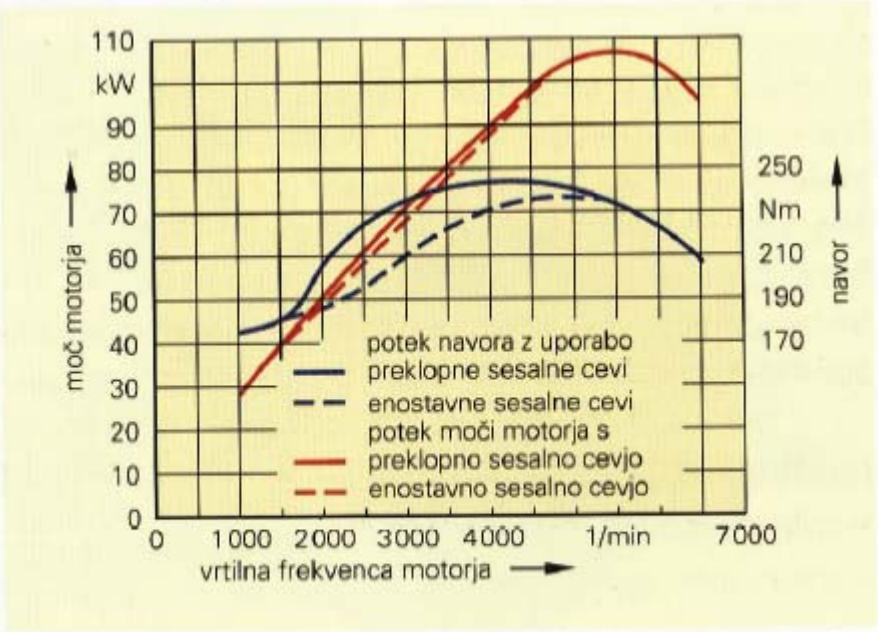

Slika 2.5.1-4: Navor in moč motorja v odvisnosti od dolžine sesalne cevi

Vir: Motorno vozilo, 2004

Tlačilka šoba

$$p_{eff} = \frac{p_1}{c_v T_1} \frac{m_f H_{LHV}}{m} \frac{\varepsilon}{\varepsilon - 1} \frac{1}{\kappa - 1} \eta$$

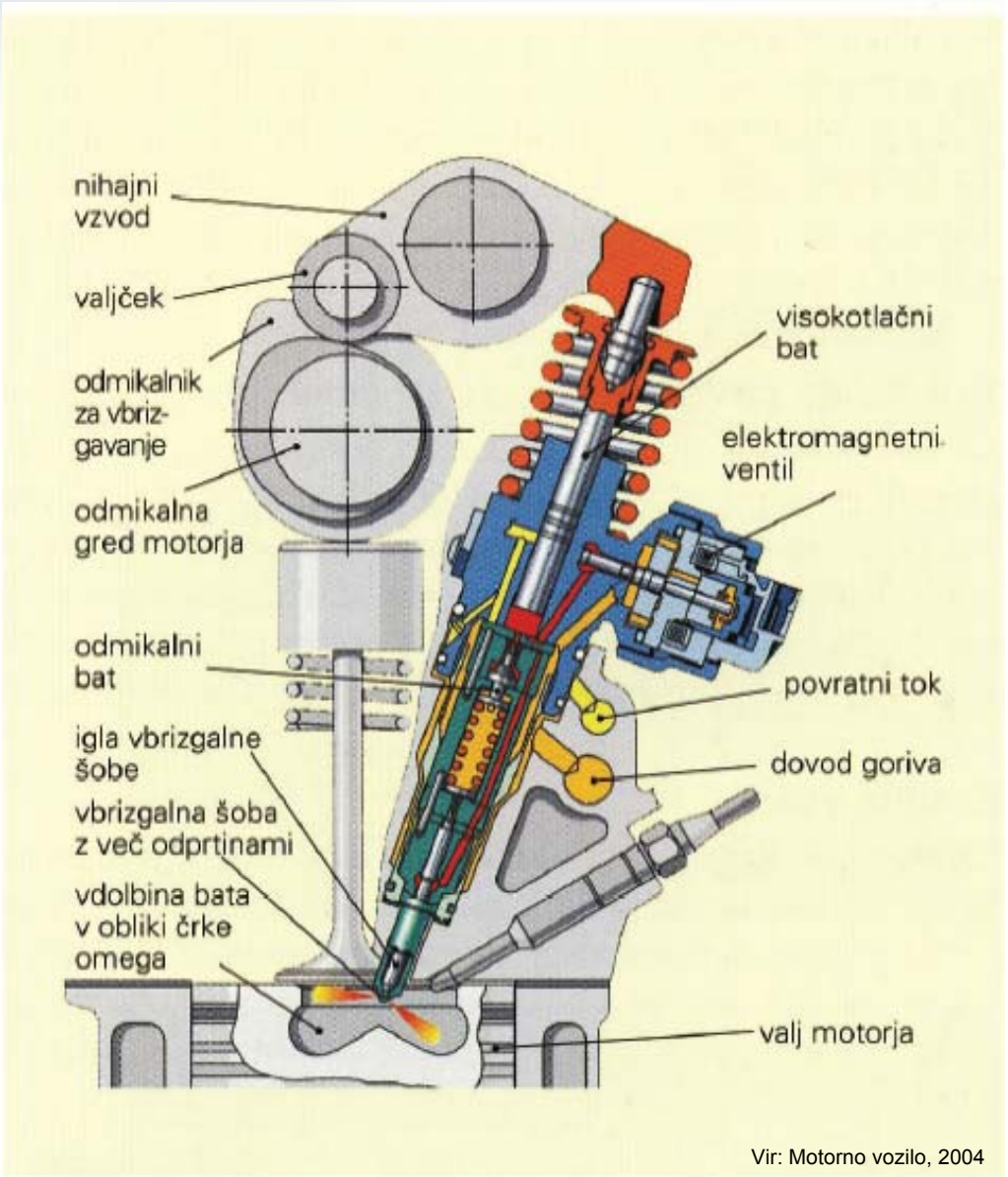

Vir: Motorno vozilo, 2004

Skupni vod

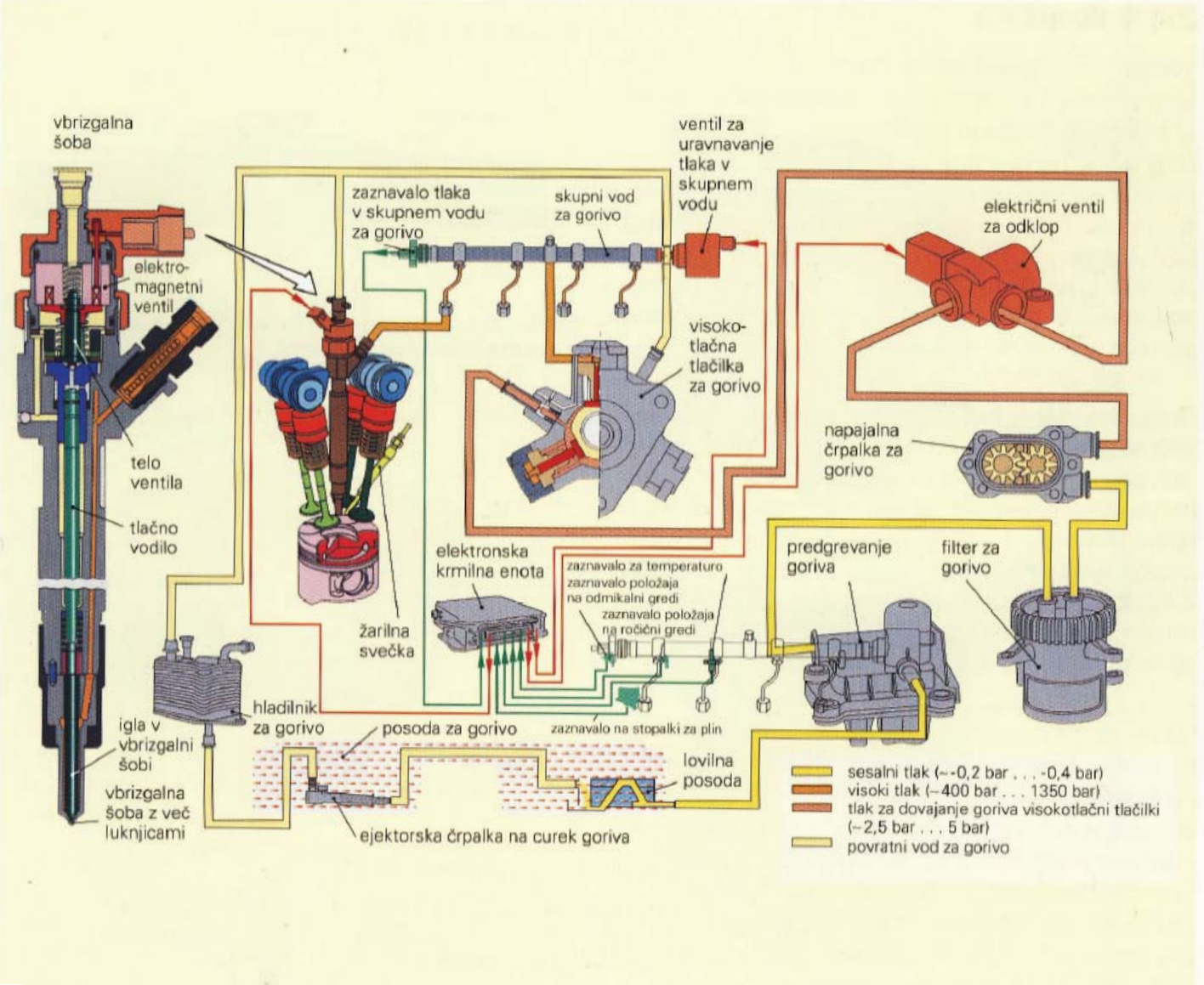

Vir: Motorno vozilo, 2004

Večkratno vbrizgavanje goriva

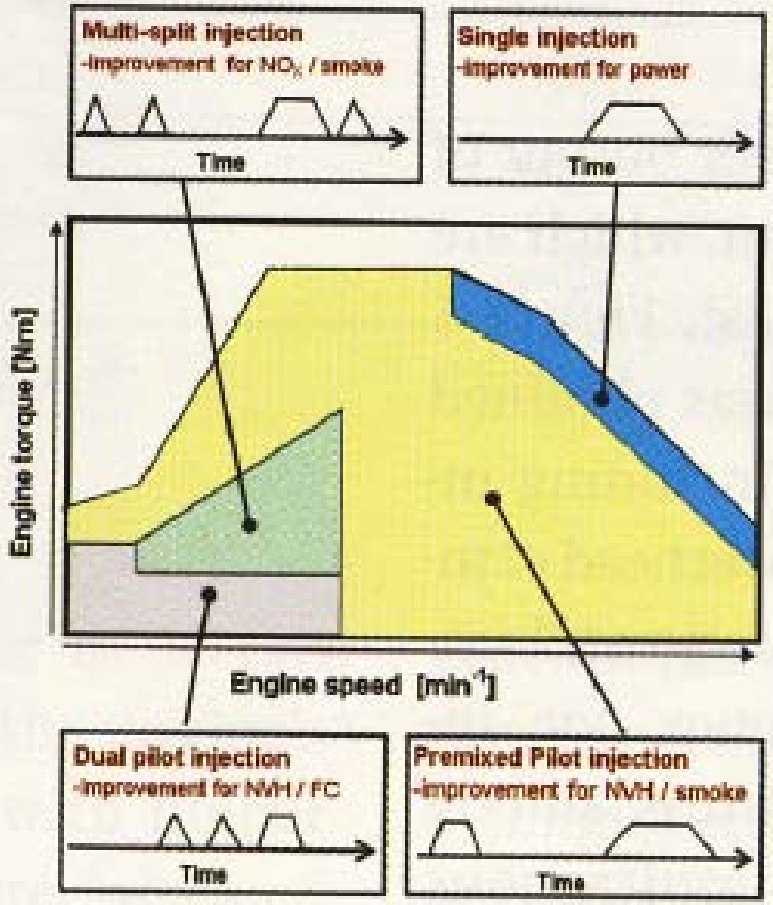

Figure 3: left: example of MBC; right: multi-injection pattern map

Vir: ATZ

Slojevito zgorevanje

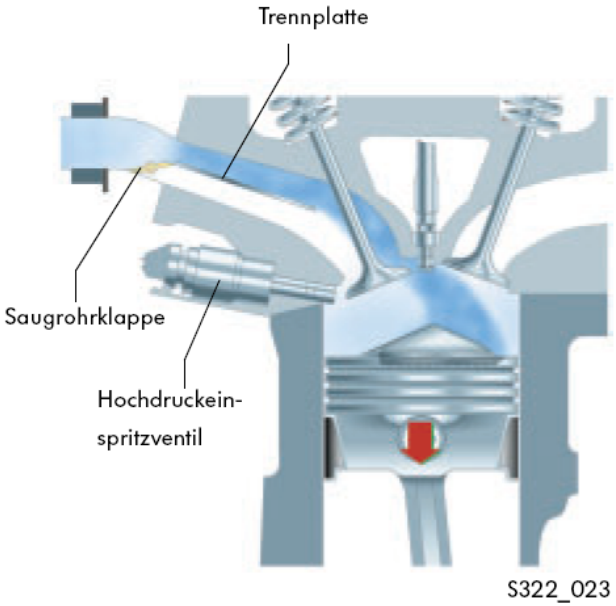

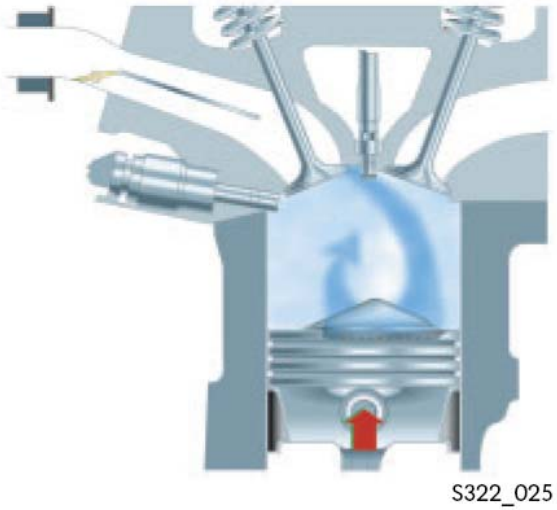

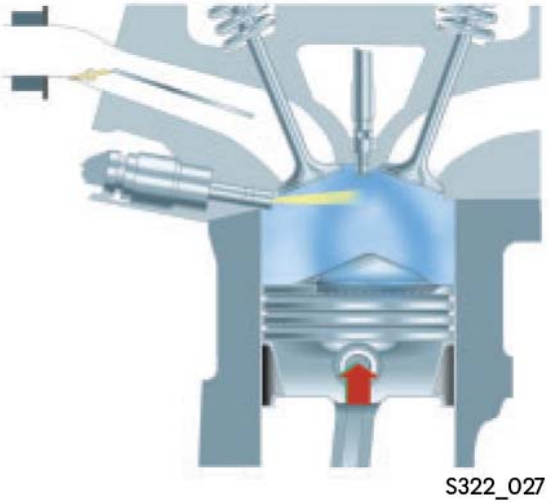

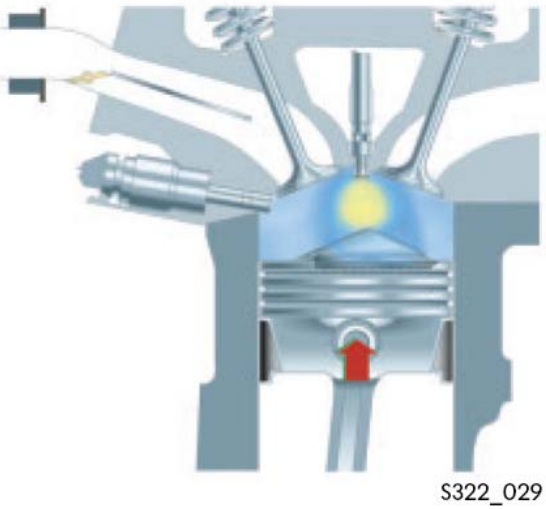

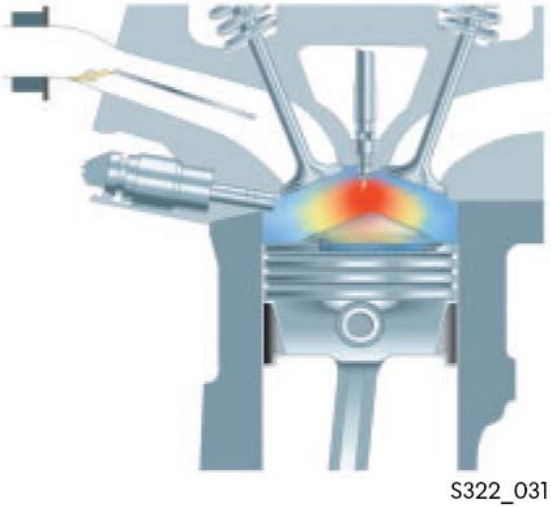

VW: Service Training, Selbststudienprogramm 322

Slojevito zgorevanje

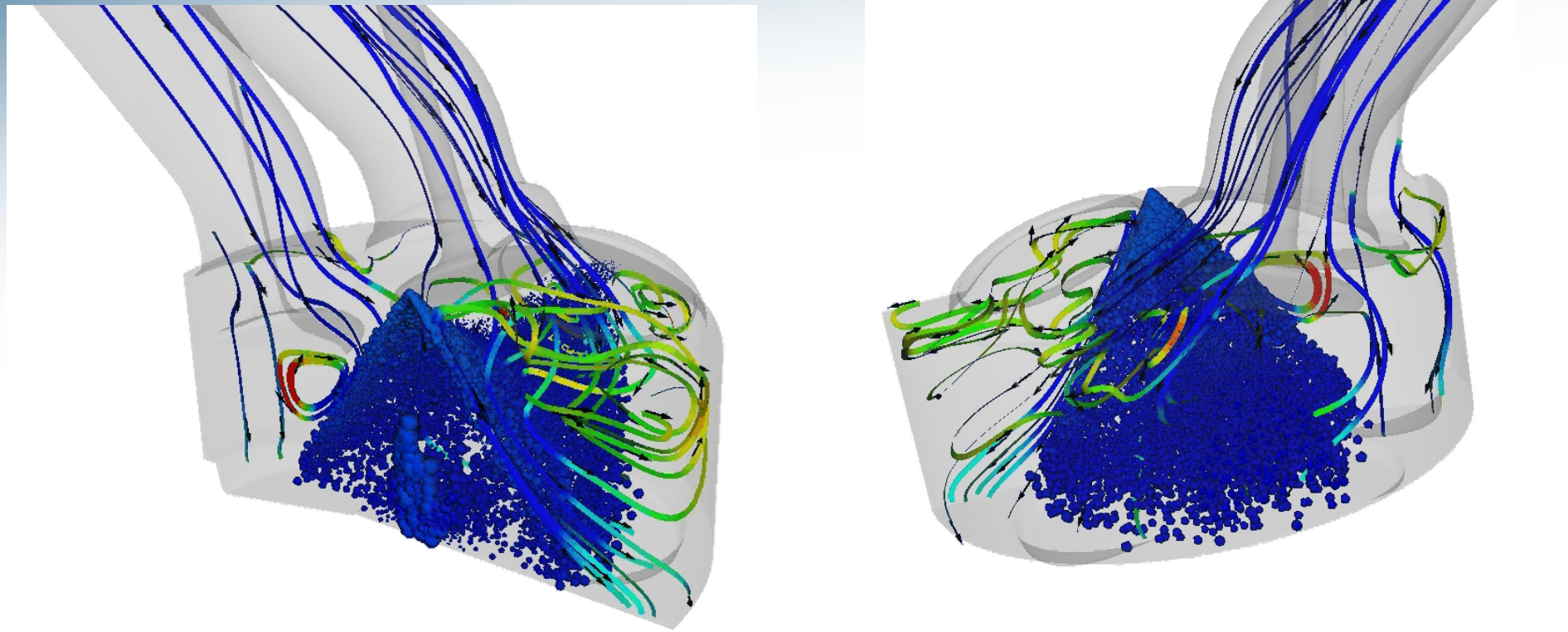

Fuel spray distribution and air-flow ribbons inside a multi-valve gasoline direct injection engine cylinder as seen from two different views. Droplets are coloured according to their temperature. Flow ribbons are colored according to air velocity component in the direction of piston movement.

www.fluid-research.com/fuel_systems.htm

Slojevito zgorevanje

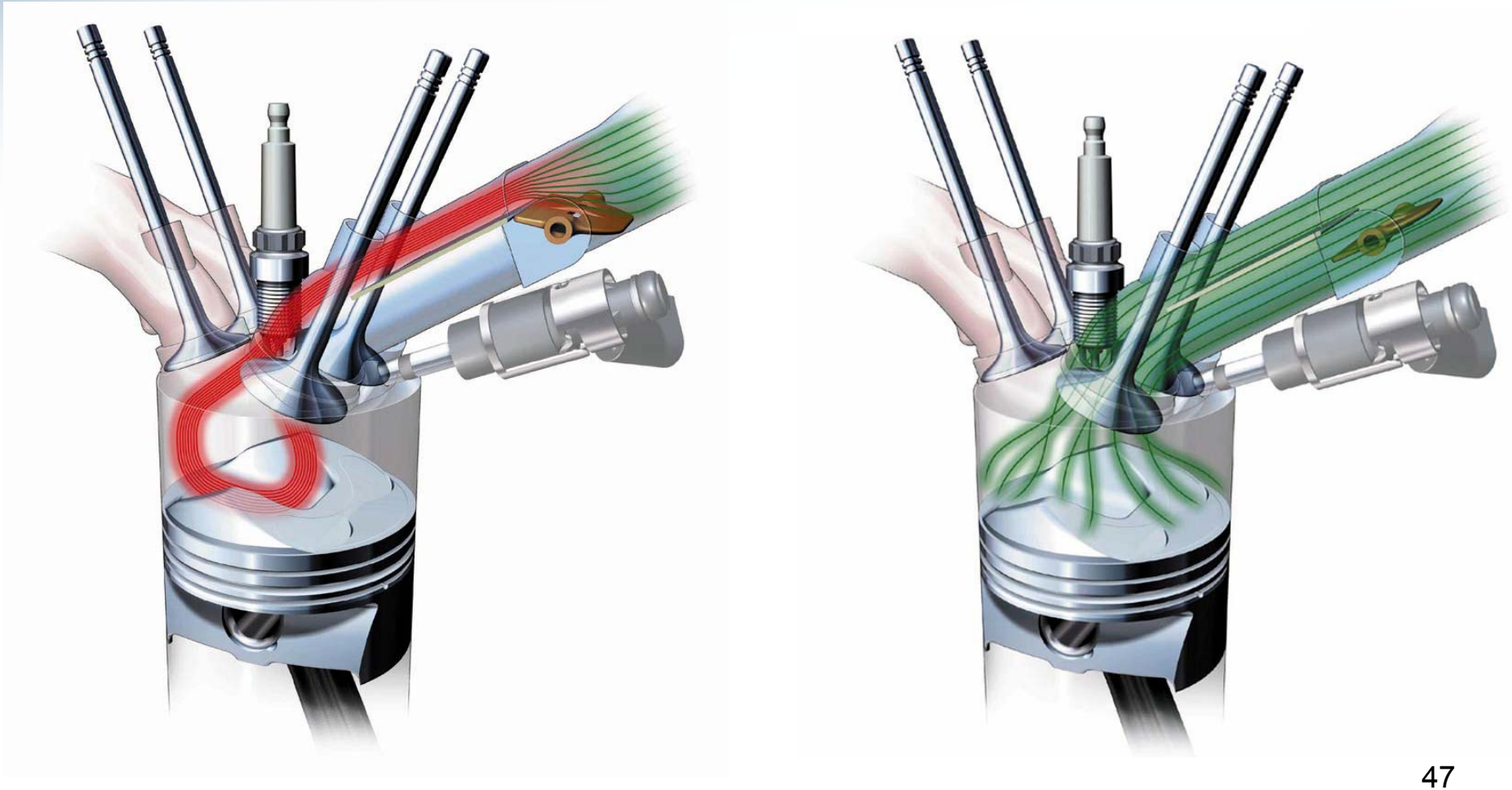

DAIMLER

Cycle and real world CO_2-emissions

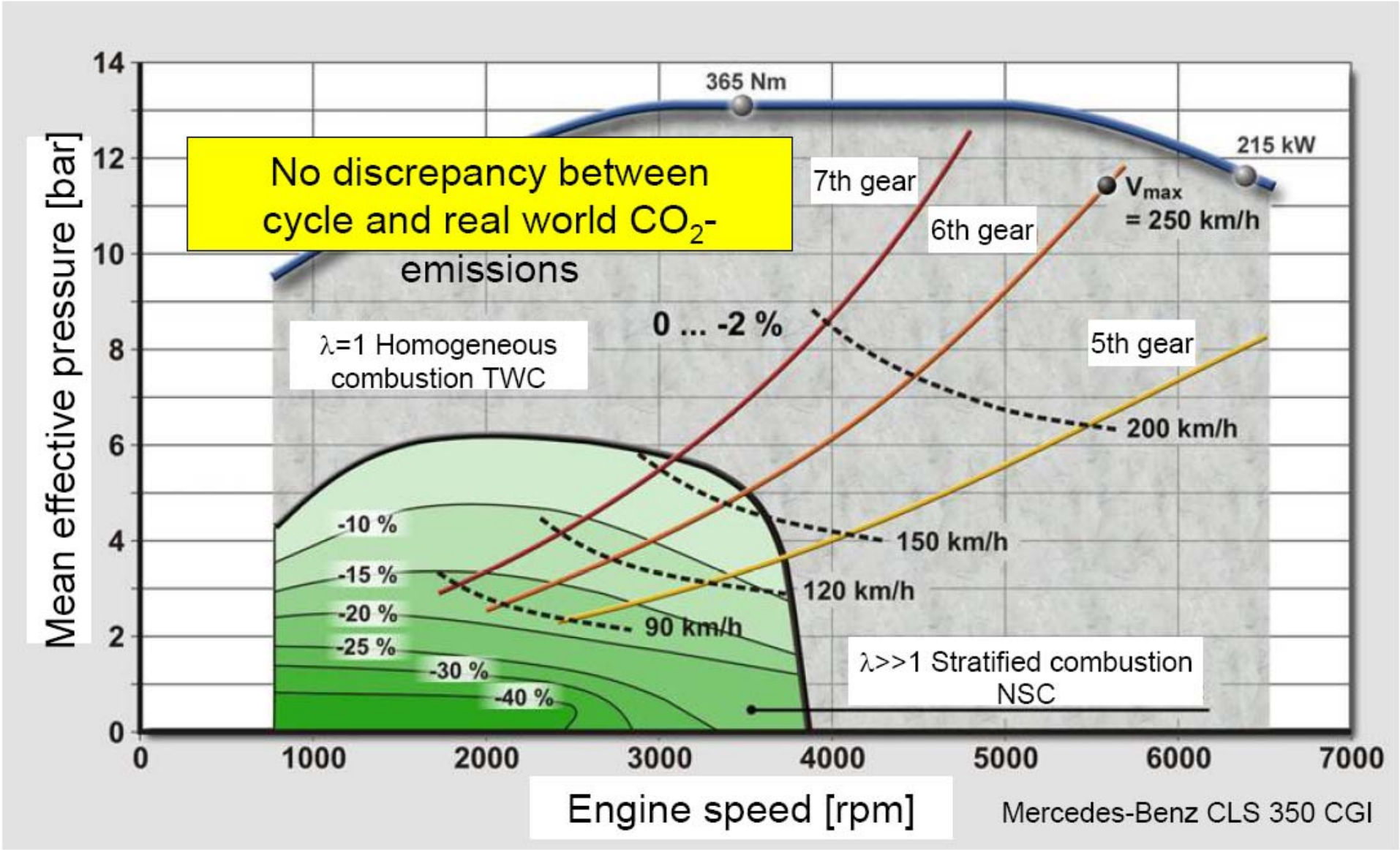

Mercedes-Benz CLS 350 CGI

HCCI – zgorevanje homogene zmesi s samovžigom

Figure 3 Injection and heat release at conventional and alternative combustion

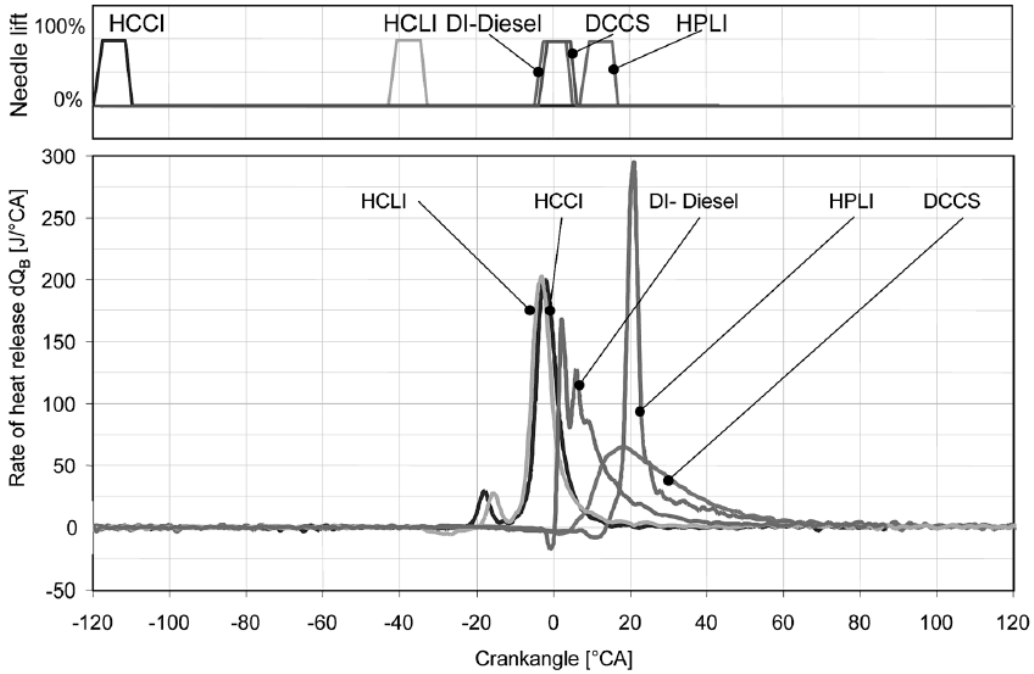

Figure 2 NO_x and soot formation as a function of local air excess ratio and flame temperature

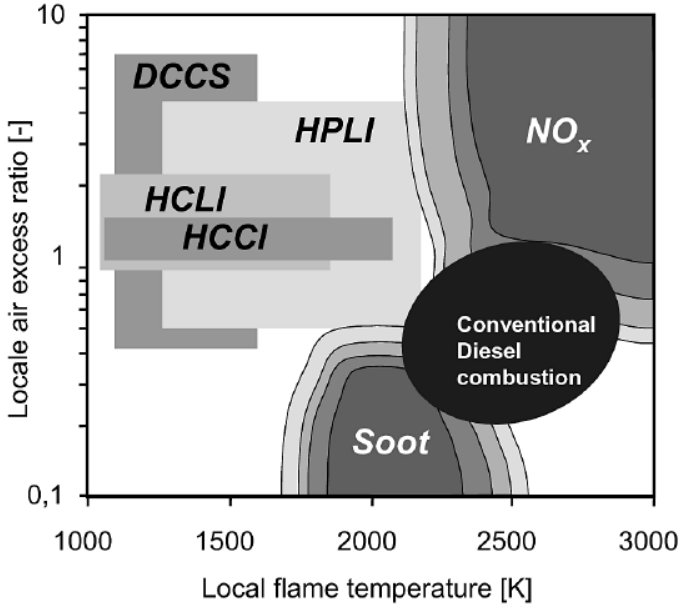

Wimmer, A et al, Potential of HCCI concepts for DI diesel engines

Pot zmanjšanja porabe goriva

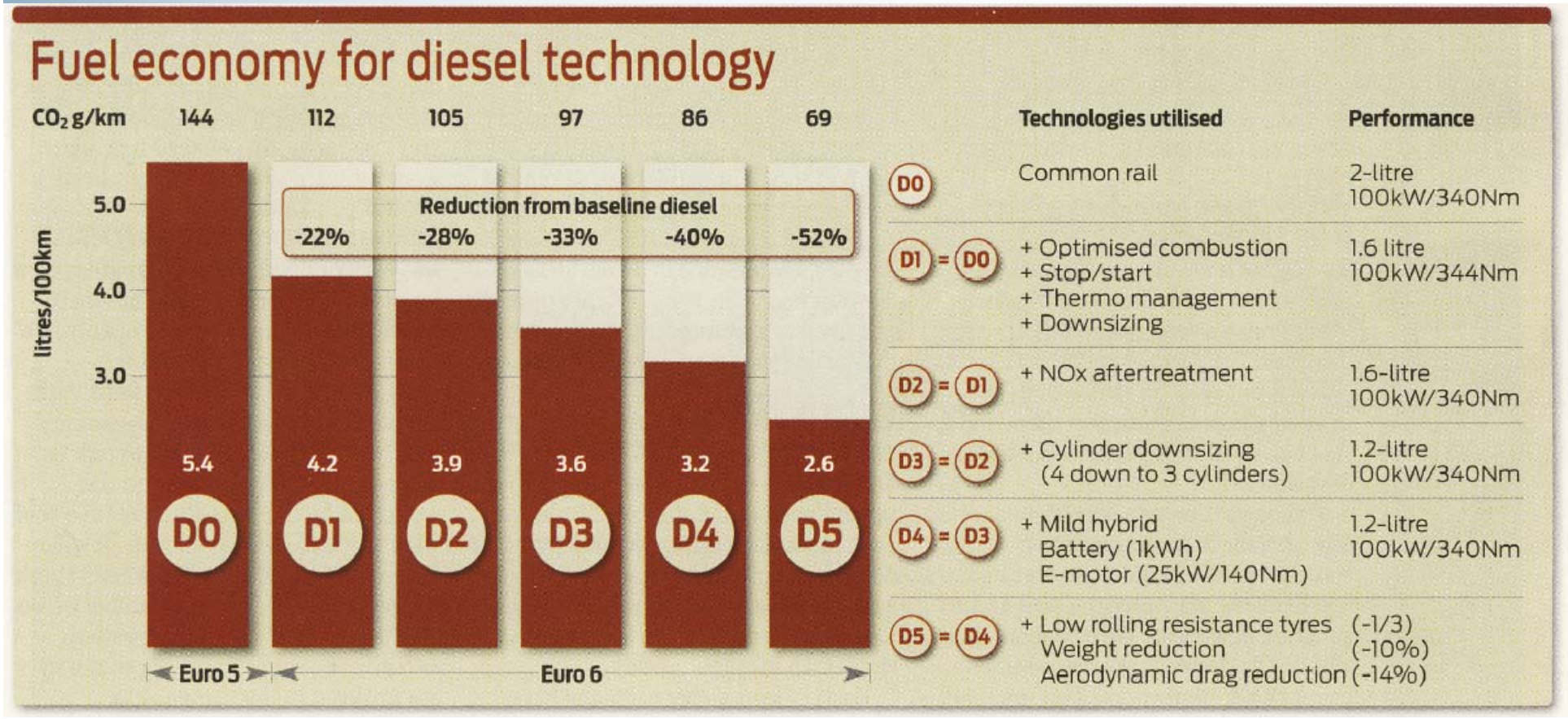

Vir: ATZ